Review of RD50 activities

RD50: Radiation hard semiconductor devices for high luminosity colliders

Marcos Fernández García[1,2]
on behalf of the RD50 collaboration

[1]Instituto de Física de Cantabria,
IFCA-Santander, Spain

[2]Visiting scientist at **CERN-EP-DT SSD** lab

VERTEX2017 – Las Caldas, Asturias (Spain) – 11-15 September 2017

RD50: it took us longer to find a logo than a rad-hard sensor for HL-LHC

(Logo by: Marko MILOVANOVIĆ)

Some other (hidden) talents in this collaboration:

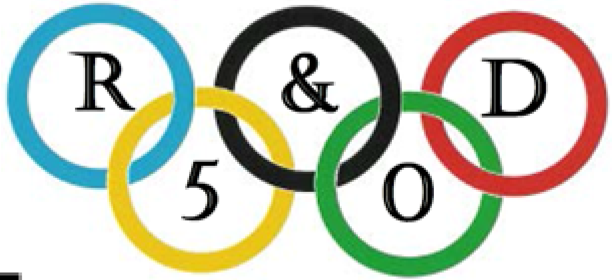

Follow this link for further artwork...

Outline of this talk

Disclaimer: *Personal choice of subjects, impossible to summarize all the activities of the collaboration*

- **RD50 introduction** …
  with focus on activities developed **only** within RD50
  - **Defect studies**
  - **New** semiconductor characterization **techniques**
  - **Fast** signal **simulators**
  - Development of **new sensors**

- Some **extra information** on:
  - **4D tracking**: UFSD and dd-APDs
  - **Acceptor removal** and its impact on LGAD, HVCMOS

This conference:
N>1 talk and 1 poster

- Selected **highlights** of last 30th RD50 workshop:
  - **HVCMOS** (bulk) radiation hardness
  - ~~**3Ds** for HL-LHC: radiation hardness~~

Backup slides
& Monday talks

- **Summary** of this summary

RD50 collaboration

RD50: Radiation hard semiconductor devices for high luminosity colliders

https://www.cern.ch/rd50/

RD50 mandate: develop and characterize semiconductor sensors for **HL-LHC**... ***and FCC?***

- HL-LHC challenge: hadron fluence of 10^{16} n_{eq}/cm^2
- FCC challenge: > 7×10^{17} n_{eq}/cm^2 `[See talk by M. Mikuz later]`

- At this moment:

  55 institutes (46 European, 7 North America, 1 Middle East, 1 Asia), **327 members**

  ...and growing

- Activities organized around **workgroups**:
  - **defect**/material characterization (DLTS and TSC measurements)
  - **detector** characterization (irradiations, IVCV, TCT, simulations,...)
  - study of **new** structures (LGAD, HVCMOS, thin detectors...),
  - **full** detector systems (LHC-like tests, timing...)

Workgroup 1: defect/material characterization

Defect studies in RD50 link **macroscopic properties to microscopic defect(s).**
Knowledge of chemical composition ⇒ deactivating harmful defects → defect engineering

Workgroup 1: defect/material characterization

Defect studies in RD50 link **macroscopic properties to microscopic defect(s).**
Knowledge of chemical composition ⇒ deactivating harmful defects → defect engineering

MAcroscopic changes: ⟶ ...due to **Microscopic ...**

- change of effective **doping**
- increase of **leakage** current
- **Trapping** of charge carriers

- **point defects**

induced by electrons, γ and charged hadrons

- **clusters**

Induced by charged hadrons and neutrons

Workgroup 1: defect/material characterization

Defect studies in RD50 link **macroscopic properties to microscopic defect(s).**
Knowledge of chemical composition ⇒ deactivating harmful defects → defect engineering

MAcroscopic changes: → ...due to **Microscopic ...**

- change of effective **doping**
- increase of **leakage** current
- **Trapping** of charge carriers

- **point defects**
induced by 60Co-γ and charged hadrons
- **clusters**
Induced by charged hadrons and neutrons

Defect/characterization methods:

Thermally Stimulated Current (TSC) and **Deep Level Transient Spectroscopy (DLTS)**:

TSC allows to calculate concentration of defects. **DLTS** gives full info (c,E_t,N_t) if Nt<<Neff0.

Measurement procedure::

TSC
1) cooling to low temperature between [10K,140K]
2) forward bias injection to fill traps
3) heating and recording of current
(i.e. emission of trapped charges)

DLTS
1) fix reverse bias, stabilize temperature
2) change occupancy of defects by
zero bias or forward bias injection
3) record capacitance transient (averaging)
(i.e. emission of trapped charges)
Do this for many temperatures to get DTLS spectrum

Macroscopic property: Vdep

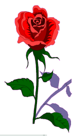

G. Lindstrom et al, NIMA 466 (2001) 308-326

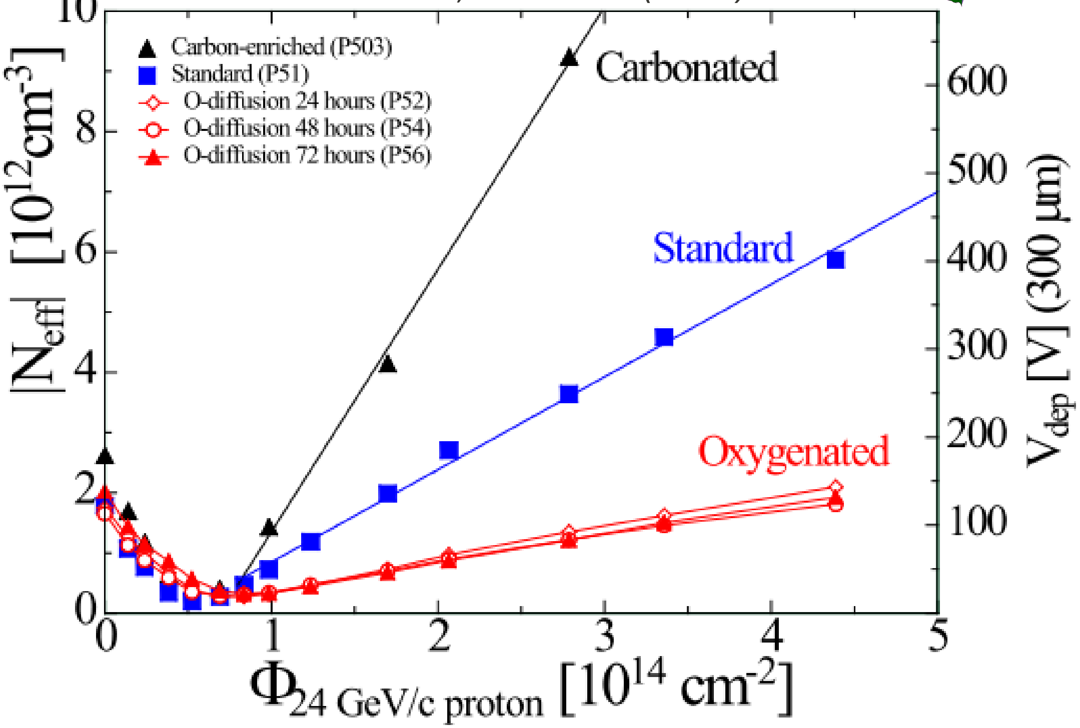

- Beneficial effect of Oxygen doping of Si wafers

- Slower increase of depletion voltage with fluence ⇒ Increased radiation hardness for charged hadrons

$$V_{dep} = \frac{q_0}{\varepsilon\,\varepsilon_0} \, |N_{eff}| \, d^2$$

Macroscopic property: Vdep

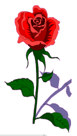

G. Lindstrom et al, NIMA 466 (2001) 308-326

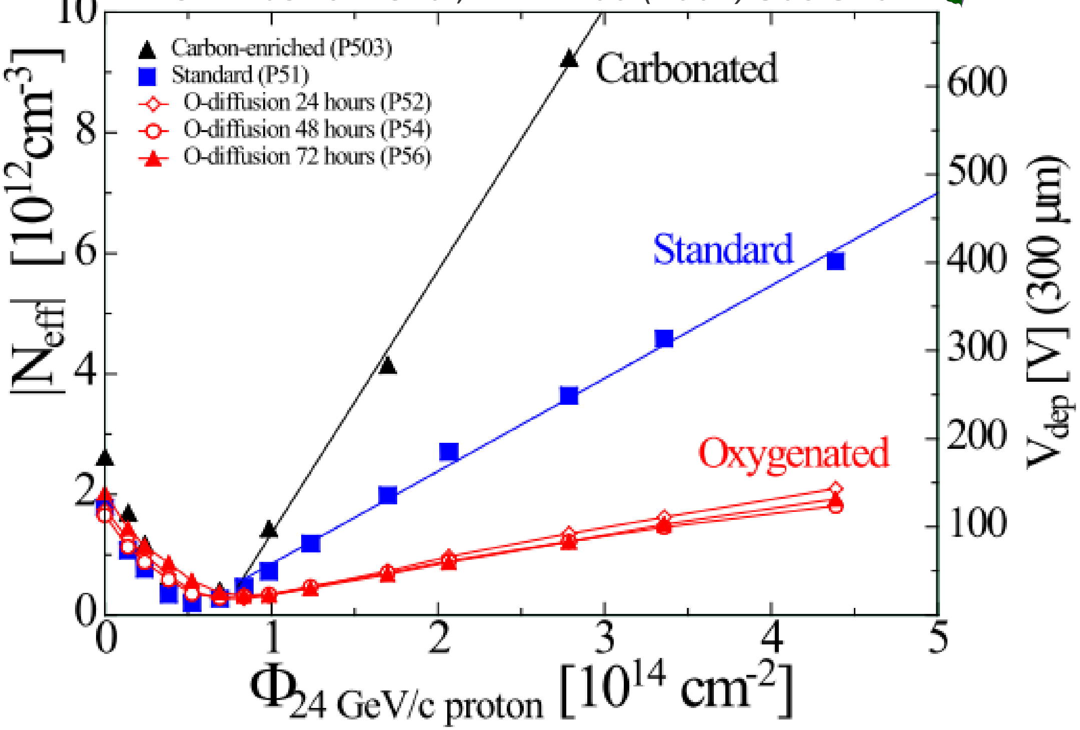

- Beneficial effect of Oxygen doping of Si wafers
- Slower increase of depletion voltage with fluence ⇒ Increased radiation hardness for charged hadrons

$$V_{dep} = \frac{q_0}{\varepsilon\,\varepsilon_0}\,|N_{eff}|\;d^2$$

Microscopical reason

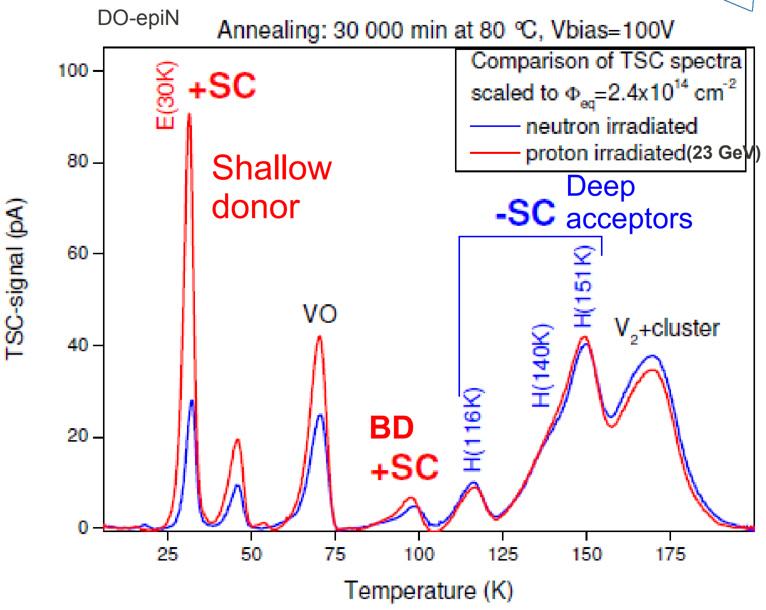

I. Pintilie, APL 92, 024101 2008

- H(116K,140K,151K) defects introduce **negative space charge** (-SC) and are responsible for type inversion of n-type material..
- In **Oxygenated** materials **E(30K)** introduces +SC and thus reduces increase of V_{dep} or even avoids type inversion.

Other defect mechanisms

VP → **Donor Removal** process (suppressed in O-rich material)

$I+B_s \rightarrow B_i$
$Bi+Oi \rightarrow BiOi$

Acceptor removal

(=Positive SC)

Workgroup 2: development of new measuring techniques

- TPA (**T**wo **P**hoton **A**bsorption) - TCT is a **new laser Transient Current Technique** to characterize **semiconductors**.
- Physical phenomena exploited is the **simultaneous absorption of 2 photons** in the material

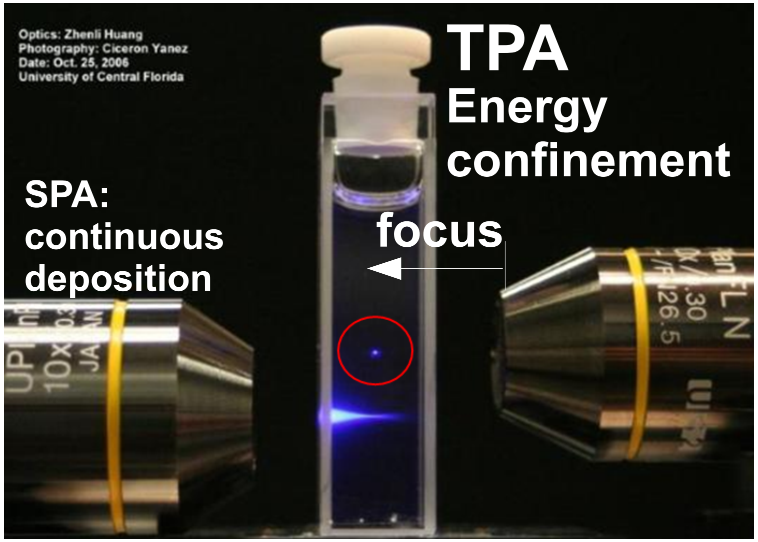

TPA in a fluorescent solution

- TPA-TCT provides a **"point-like"** carrier generation volume: 3D spatial resolution

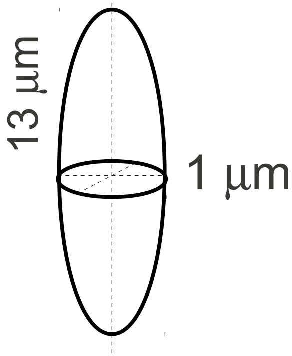

M.Fernandez, NIMA Volume 845 (2017) 69-71

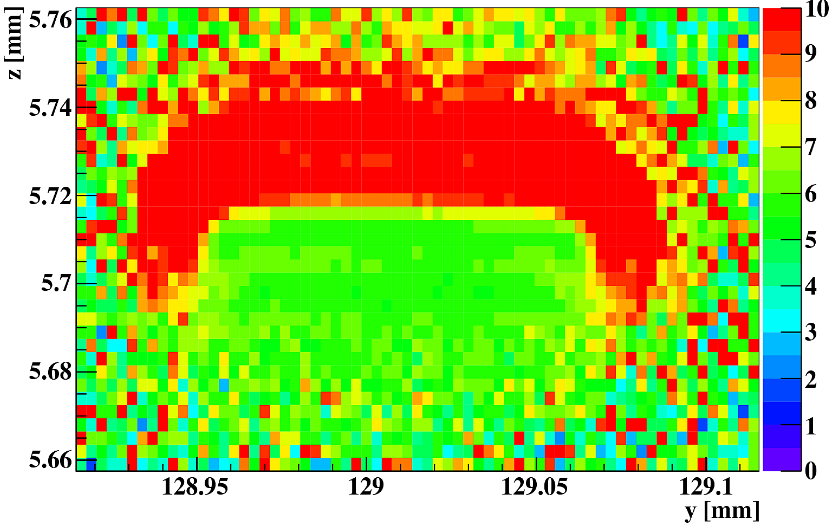

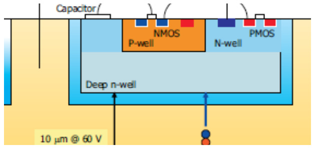

Standard TCT

λ=1064 nm, σ=10 μm, **200 ps**-pulsed laser

HVCMOS (CCPDv3) Showing: Collection time map

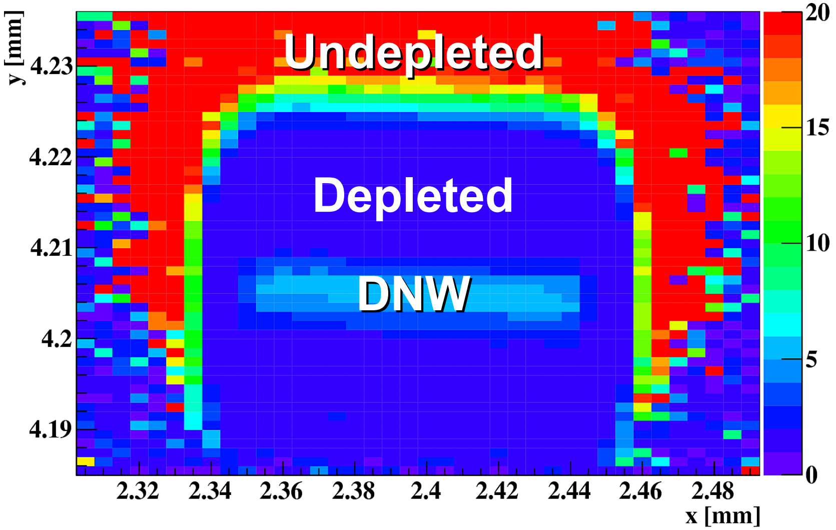

TPA-TCT

λ=1300 nm, σ=1 μm, **200 fs**-pulsed laser

Two Photon Absorption TCT

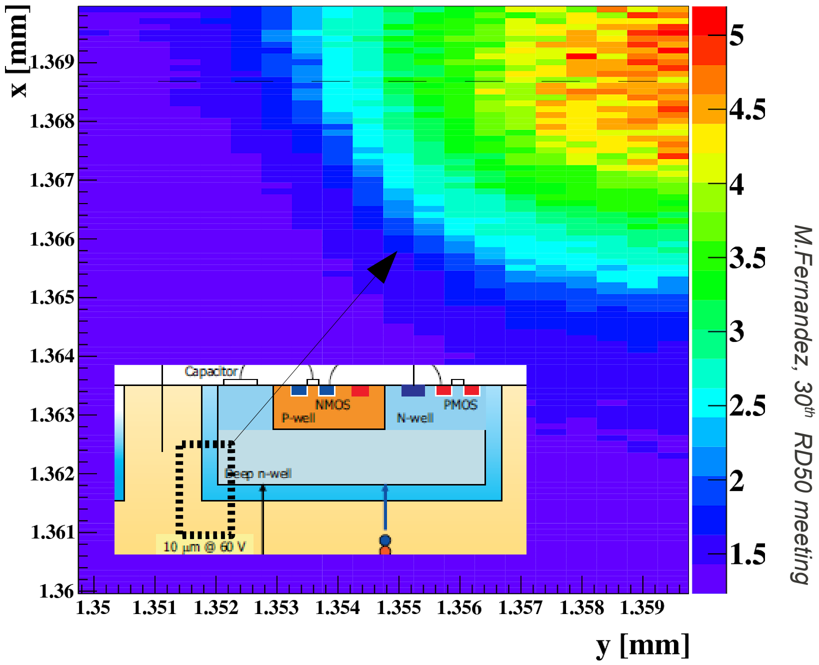
Coll. Time zoom on HVCMOS DNW

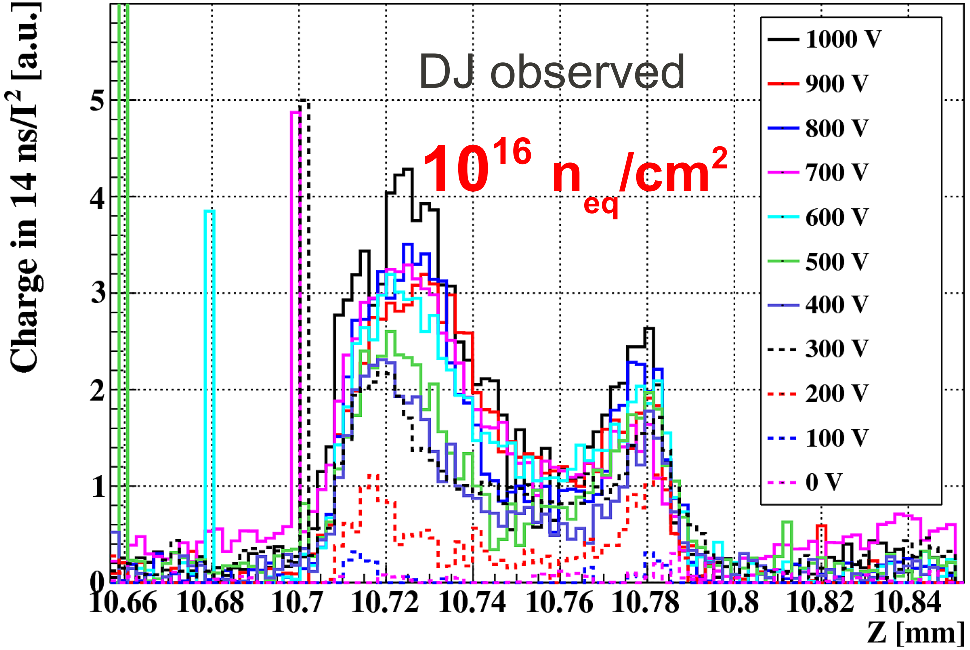
CNM PiN diode

M.Fernandez, 28th RD50 meeting

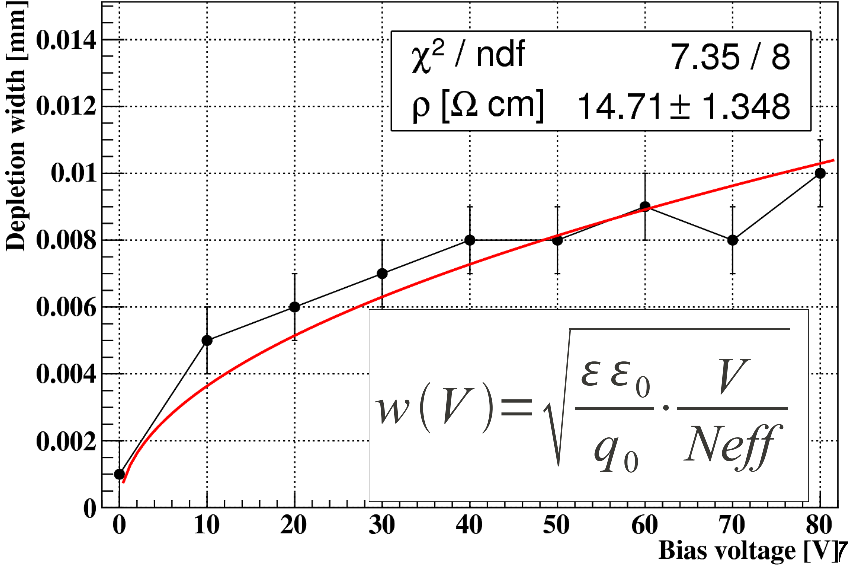
HVCMOS: bulk doping calculation

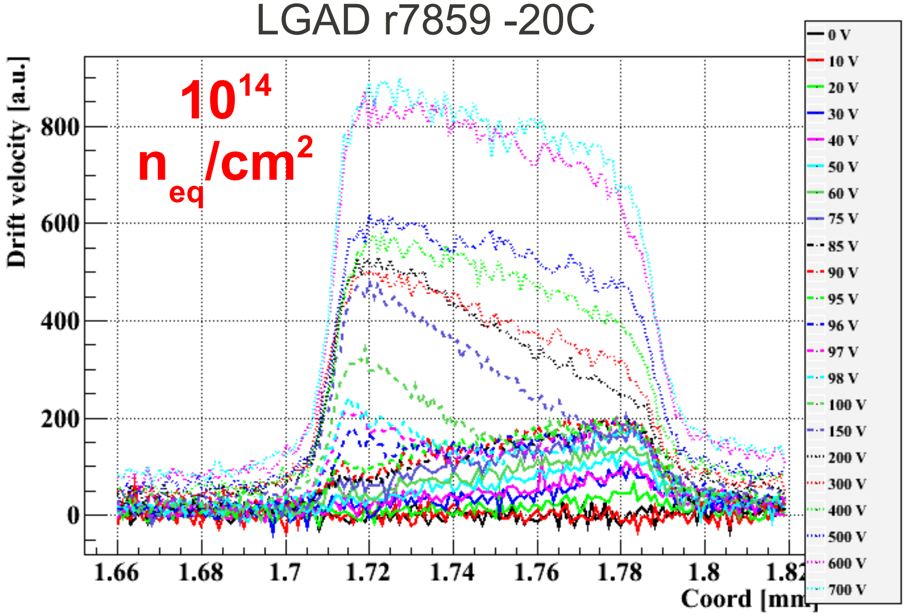
LGAD r7859 -20C

Workgroup 2: development of fast signal simulators

- **Commercial TCAD** simulation tools are the state of the art in simulation of physical processes in Si. However, **radiation damage** is not natively included. Because of **convergence problems** of this tool, only a reduced number of effective defect levels is used (**2-3 levels** max).

- Simulations are **tuned** to reproduce detectors/measurements (for instance IV/CV). The agreement with **different** measurements (CCE, for instace) is **qualitative**. Still, this is good **enough** for **optimization** of designs and **projections** performance.

- Inside RD50, three specialized **fast simulators** have been developed, which are mostly used to reproduce TCT measurements but also to optimize detector geometries Common **features**:
    - Charge **carriers** are “**imported**” from parametrizations (GEANT, optical models...)
    - **Space charge** is implemented via Neff parametrization
      Irradiated devices include (effective) trapping and Double Junction models
    - Signal (induced current) is calculated via **Ramo's theorem**
      weighting field and **electric field** are solved using **FEM**
    - Charge transport by **drift** and **diffusion**
    - **Electronics shaping** included
    - Code is **open**

- See RD50 talk on cross calibration of the different tools here

Workgroup 2: development of fast signal simulators

[Click on the name of the software to go to its webpage]

KDetSim

IJS Ljubljana

- **ROOT** shared library
- **Scripted**

- **True 3D simulation**

- It is the **most flexible**. Accepts any **arbitrary geometries** Diodes, strips, HVCMOS, 3D...

- Impact ionization, trapping, drift and diffusion

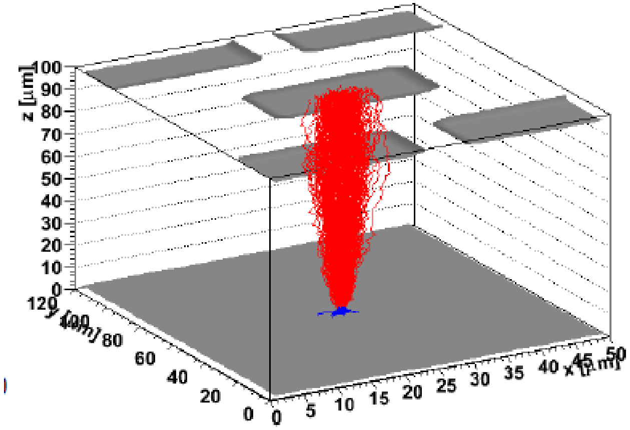

WeightField2

INFN Torino

- **GUI** based
- Built on **ROOT**
- It simulates **diodes** and **strips**
- Development has followed that of **LGADs** and **UFSD**
- **Drift, diffusion, impact ionization**
- Graphical display of charge carriers motion
- Impressive agreement to measured UFSD data

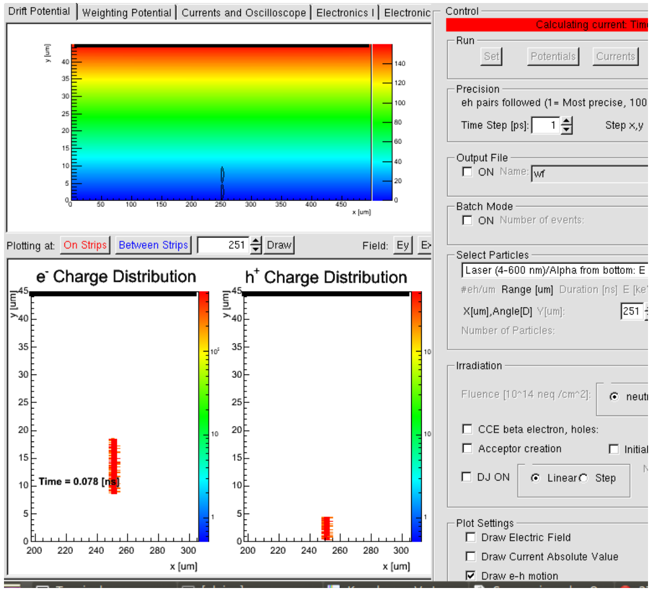

Precision
eh pairs followed (1= Most precise, 100
Time Step [ps]: 1
Step x,y
Output File
☐ ON Name: wf
Batch Mode
☐ ON Number of events:
Plotting at: On Strips Between Strips 251
Select Particles
Laser (4-600 nm)/Alpha from bottom: E
#eh/um Range [um] Duration [ns] E [ke
X[um],Angle[D] Y[um]: 251
Number of Particles:
Irradiation
Fluence [10^14 neq /cm^2]: ● neutr
☐ CCE beta electron, holes:
☐ Acceptor creation ☐ Initial
☐ DJ ON ● Linear ○ Step
Plot Settings
☐ Draw Electric Field
☐ Draw Current Absolute Value
☑ Draw e-h motion

TRACS

IFCA & CERN

- **GUI and CLI** available (callable from **user source** code)
- Uses 3rd party libraries for FEM calculations
- Simulation of **diodes** and **strips**
- Main goal is to **fit parameters** (Neff, trapping) to data. Interface to MINUIT.
- Makes intensive usage of **parallel computing**

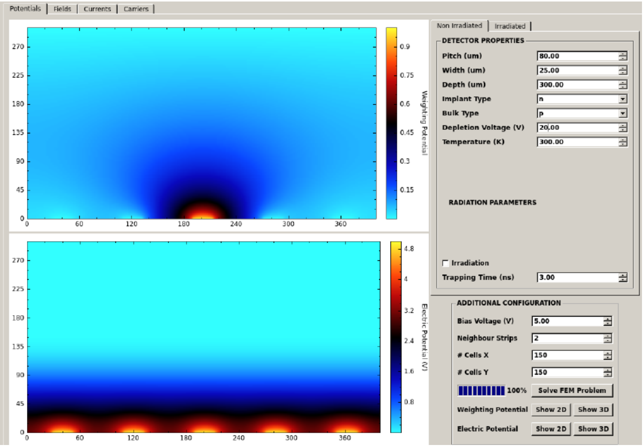

DETECTOR PROPERTIES
Pitch (um) 80.00
Width (um) 25.00
Depth (um) 300.00
Implant Type n
Bulk Type p
Depletion Voltage (V) 20.00
Temperature (K) 300.00
RADIATION PARAMETERS
☐ Irradiation
Trapping Time (ns) 3.00
ADDITIONAL CONFIGURATION
Bias Voltage (V) 5.00
Neighbour Strips 2
Cells X 150
Cells Y 150
100%
Weighting Potential
Electric Potential

Workgroup 3: new structures – Low Gain Avalanche Diodes

- **LGAD**s proposed&developed at **CNM-Barcelona** within **RD50**. First RD50 report by **2010**. **Today**, 4 suppliers: **CNM**, **FBK**-Trento and **HPK**-Japan, Micron Ltd..

  2016: 50 µm LGADs for CMS-TOTEM PPS

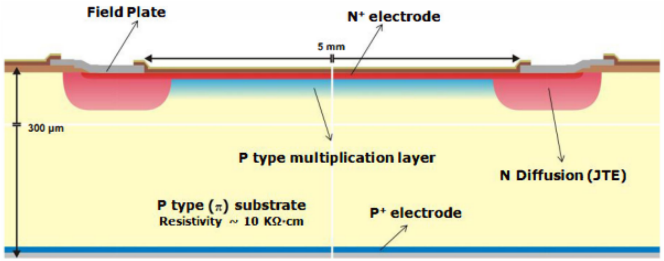

P.Fernandez, PhD thesis

- Devices exploit **impact ionization** (charge multiplication in high field regions) to achieve **faster** (→ improve **timing** performance) and radiation **harder** (→ **trapping** mitigation) sensors.

- Obtaining **low gain is challenging**: it implies controlling the doping layer concentration to a few percent

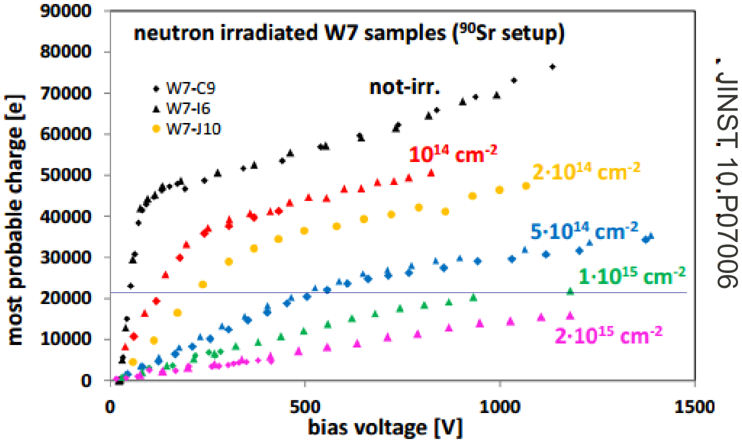

G. Kramberger 2015 , JINST 10,P07006

- **Radiation hardness** actively studied by **RD50**:

  Irradiations → **characterization** → TCAD and Weightfield2 simulations → **Optimization** → **Production** → **Measurement**

- LGAD **gain decrease** with increasing **radiation** (B-acceptor removal). Solutions:
  1) **Thin** layers
  2) **Defect engineering**:
     Ga-implanted gain layer
     Carbon co-implantion to Boron (prevents B-removal)

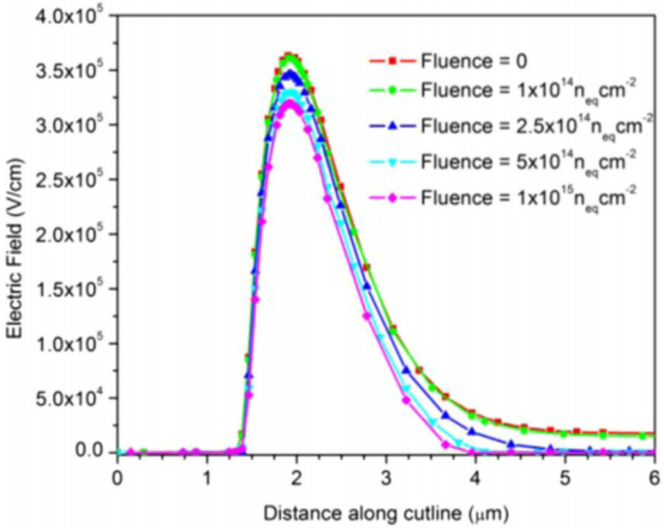

R. Dalal NIMA 836 (2016) 113–121

Workgroup 3: Ultra Fast Silicon Detectors for timing applications

- Timing at HL-LHC requires **separating** different events within **same bunch crossing**. With high **pile-up**, time distribution of events per bx is a gaussian with a **width of ~150 ps**..
⇒ **~30 ps** resolution **needed** to discriminate events inside a bx.

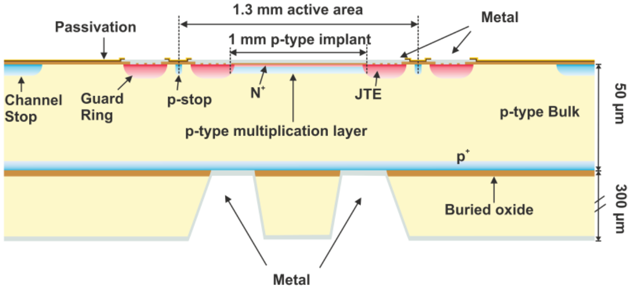

- **A realization** of silicon devices for timing **at HL-LHC** has led to **thin LGADs**. These devices are called UFSD and provide **4-Dimensional Tracking** (position+time)

- **Why is gain interesting for timing?**
Time is measured when the signal crosses a threshold.
Detectors with **gain** have **faster slew** rate

- **Why low gain?**
Low gain ⇒ low **noise** (lower excess noise factor)
Low gain ⇒ lower **power** consumption after irradiation
Low gain ⇒ lower **fields**, easier segmentation
High gain ⇒ **early BD** when operating them **cold**.
Not possible apply enough bias to reach saturated vdrift.

See: H. Sadrozinski
arXiv:1704.08666v4
&
Poster by G. Pellegrini
(this conference)

- **Why thin?**

Rise time for a MIP is determined by the **drift time** of an electron traversing the thickness

It was found that **gain** reduction after irradiation can be **recovered** by increasing bias **voltage** } This is **easier** in **thin** detectors: $\mathbf{V_{dep} \propto d^2}$

UFSD for timing applications

- **Why low gain?**
  - No improvement in time resolution for G≥15
  - Shown HPK UFSD, 45 μm thick and at 3 different T
  - **Jitter decreases** as G increases, while **Landau** fluctuations (non-uniform charge depositions) **saturates**

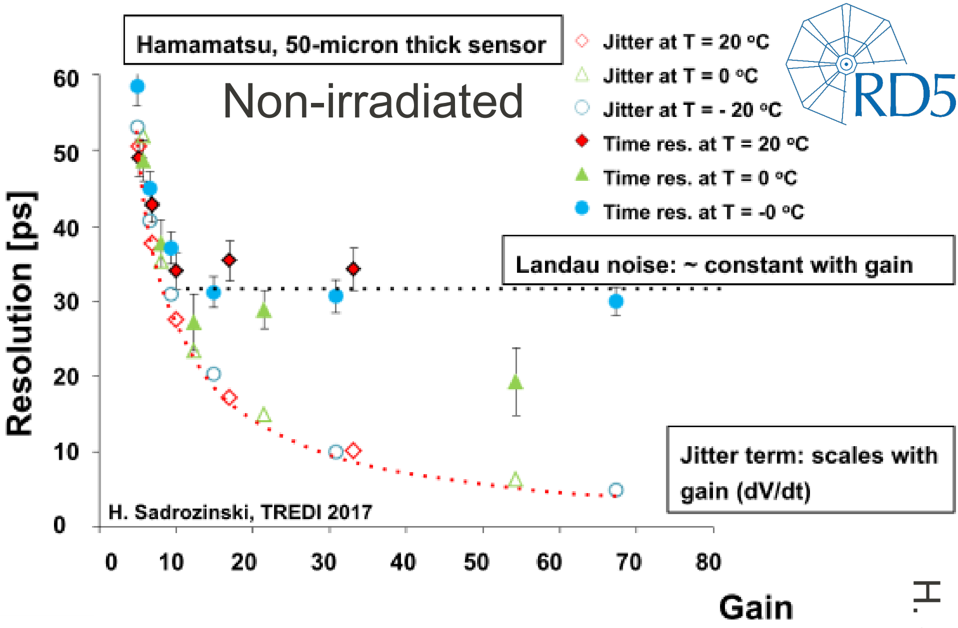
Hamamatsu, 50-micron thick sensor

Non-irradiated

Landau noise: ~ constant with gain

Jitter term: scales with gain (dV/dt)

H. Sadrozinski, TREDI 2017

- **Why thin?**

While...

Max. signal	$I_{max} \propto n_{e-h} G q_0 v_{sat}$	Signal amplitude independent of thickness
Slew rate	$\frac{di_{gain}}{dt} \sim \frac{dV}{dt} \propto \frac{G}{d}$	Thin is faster

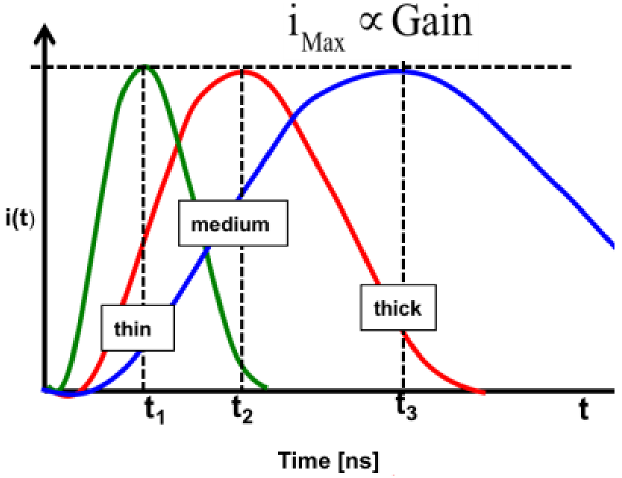

H. Sadrozinski arXiv:1704.08666v4

- **Landau noise** (due to non-uniform creation of e-h pairs along the trajectory) does **not depend on Gain** and is higher for thicker sensors

WF2 Simulation
Time uncertainty due to Landau non-uniform charge deposition
BBA amplifier, G ~ 20, various thicknesses

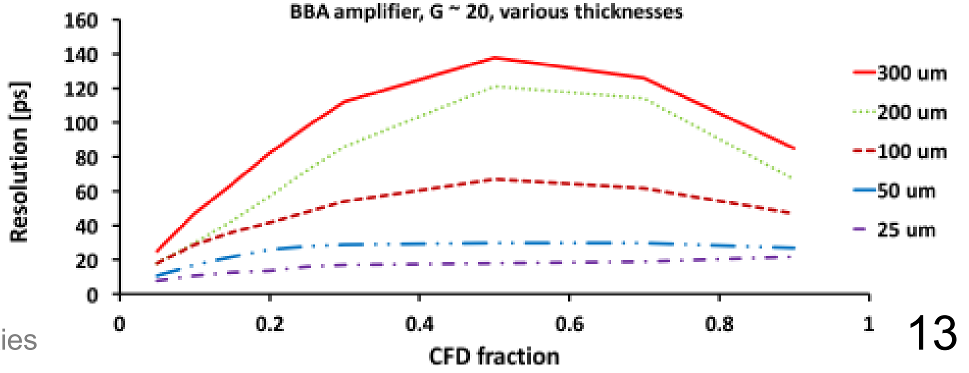

UFSD radiation hardness

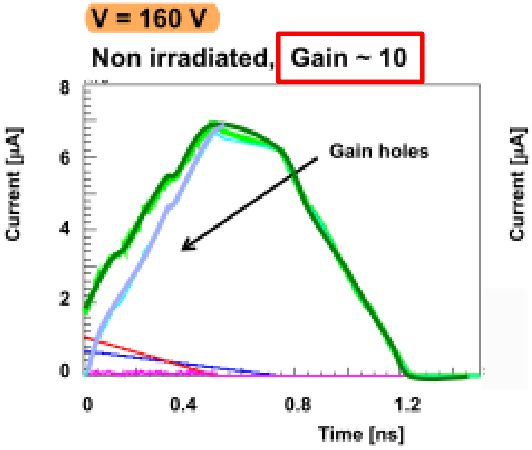

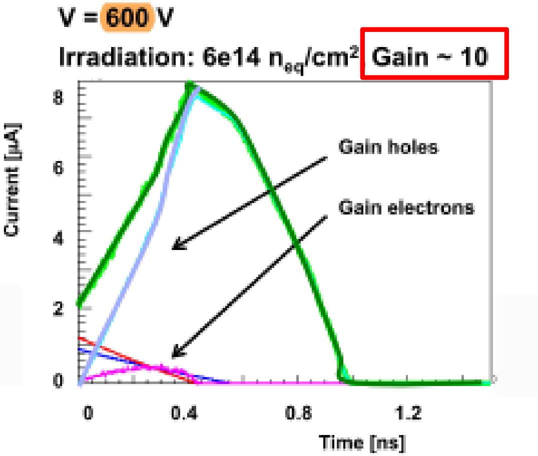

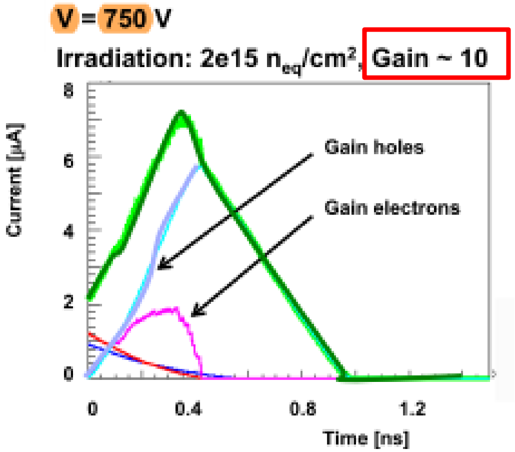

WeightField2: Gain restoration achieved via **increase** of bias **voltage**

H. Sadrozinski arXiv:1704.08666v4

- **Because of radiation damage,** multiplication layer gets deactivated but breakdown limit rises. Applied bias is enough for **CM to occur in the bulk**.

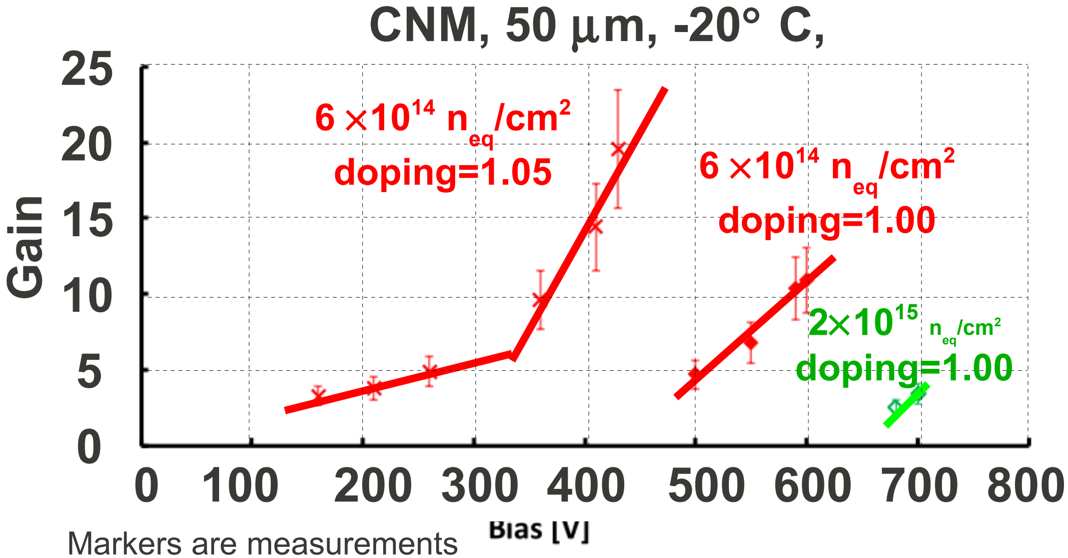

Markers are measurements
Lines only to guide the eye

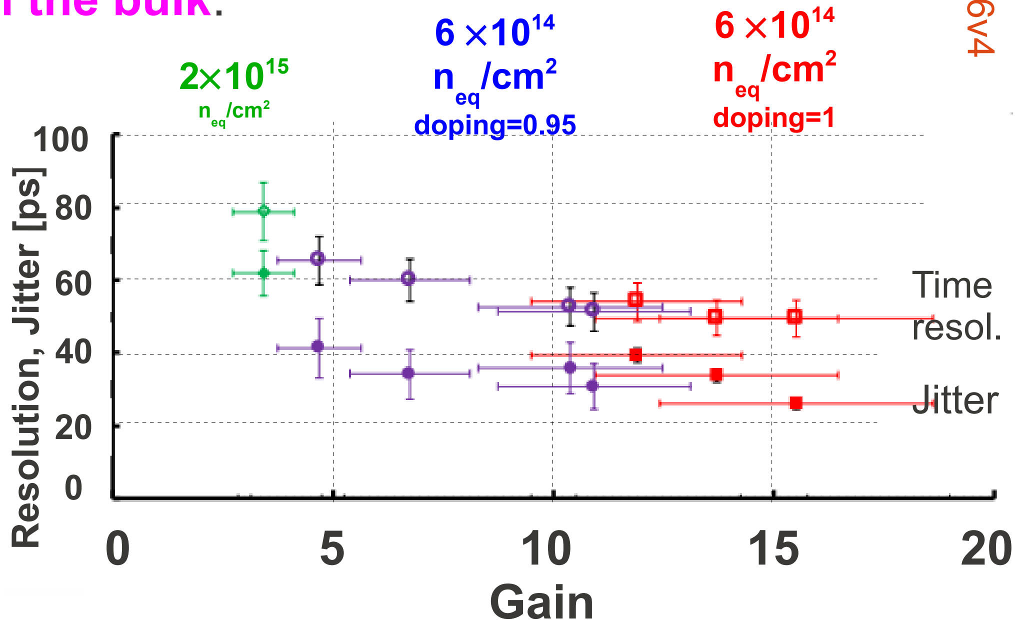

UFSD@2017: 80 ps time resolution at 2×10^{15} neq/cm^2 with a gain~5

Deep Diffused APDs for timing

- Produced by **R**adiation **M**onitoring **D**evices (RMD), 1800 V, ≤280 μm, Gain~500

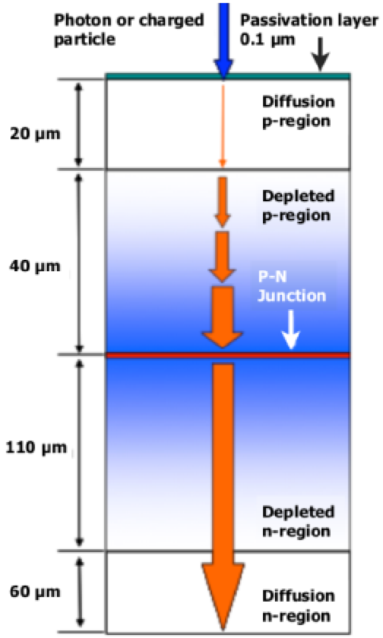

Depletion region does not touch top and bottom surfaces

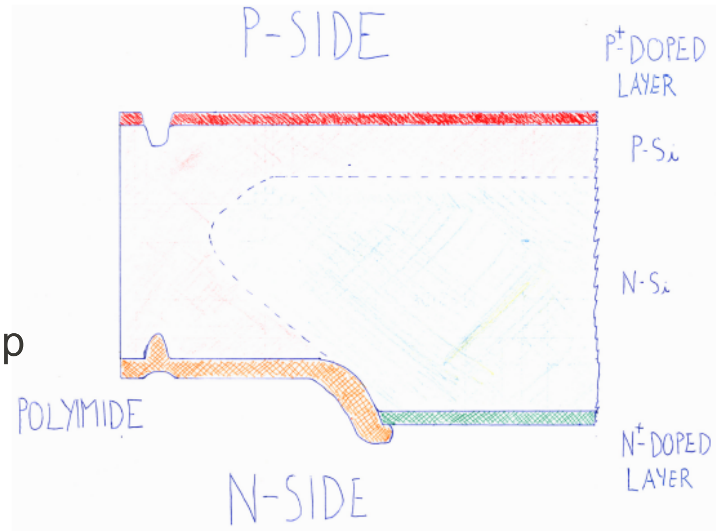

Electric field at 1700 V:

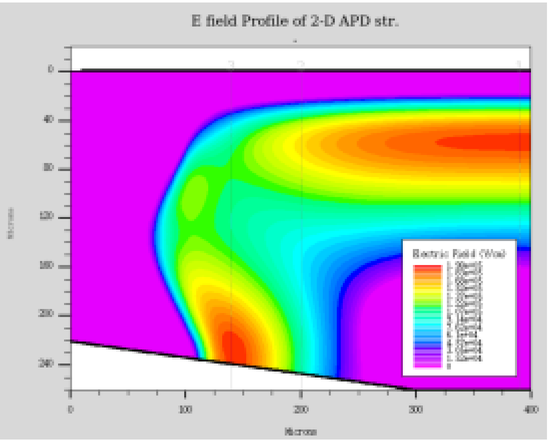

TCAD simulation by R.Dalal,

M. Centis Vignali, 30th RD50

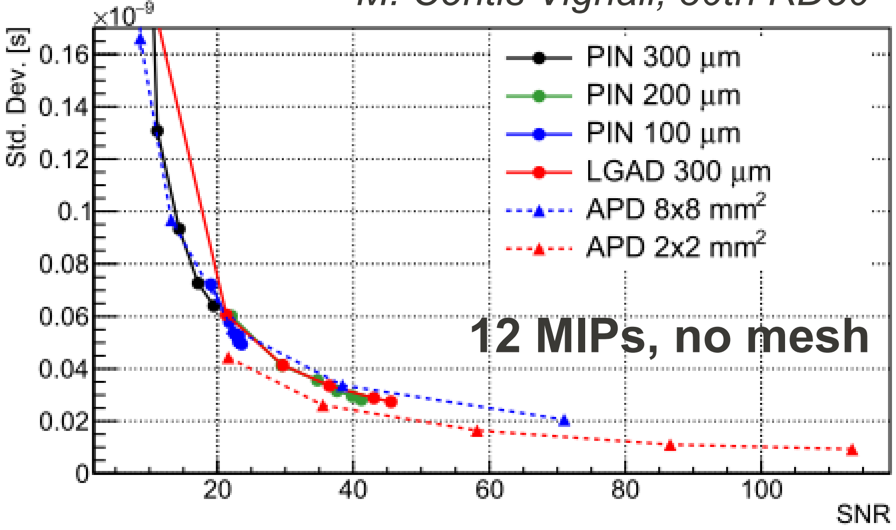

12 MIPs, no mesh

Time resolution was **improved** applying a metal mesh on top of the detector (isolated by Kapton layer)

Measurements with laser show **9 ps** time resolution, for an **unirradiated** sensor operated at **1800 V**.

Deep Diffused APDs for timing

- Produced by **R**adiation **M**onitoring **D**evices (RMD), 1800 V, ≤280 µm, Gain~500

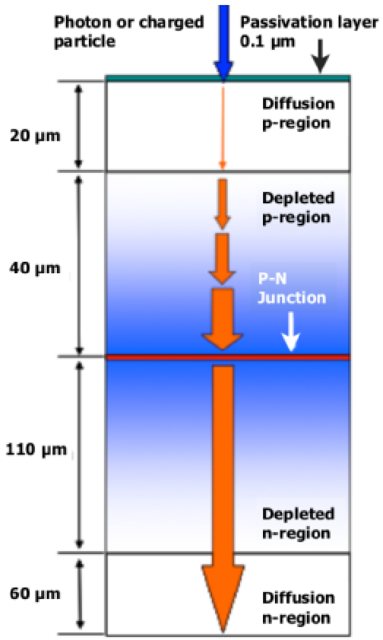

Depletion region does not touch top and bottom surfaces

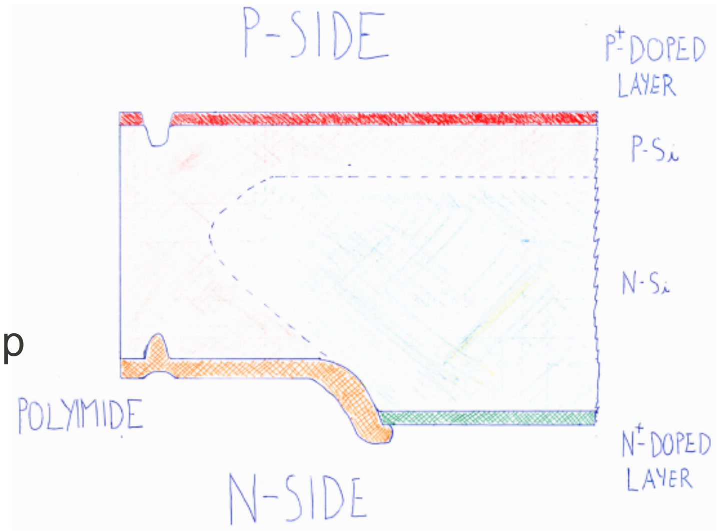

Electric field at 1700 V:

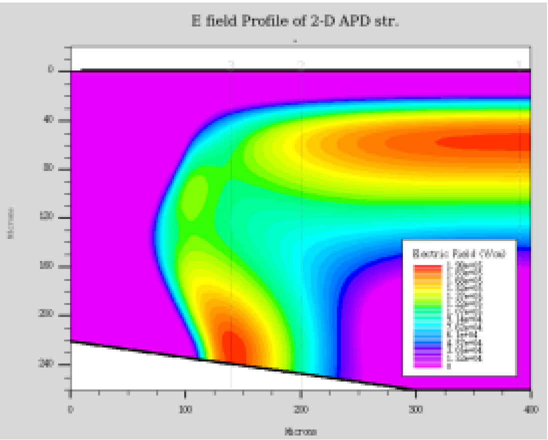

TCAD simulation by R.Dalal,

M. Centis Vignali, PSD11

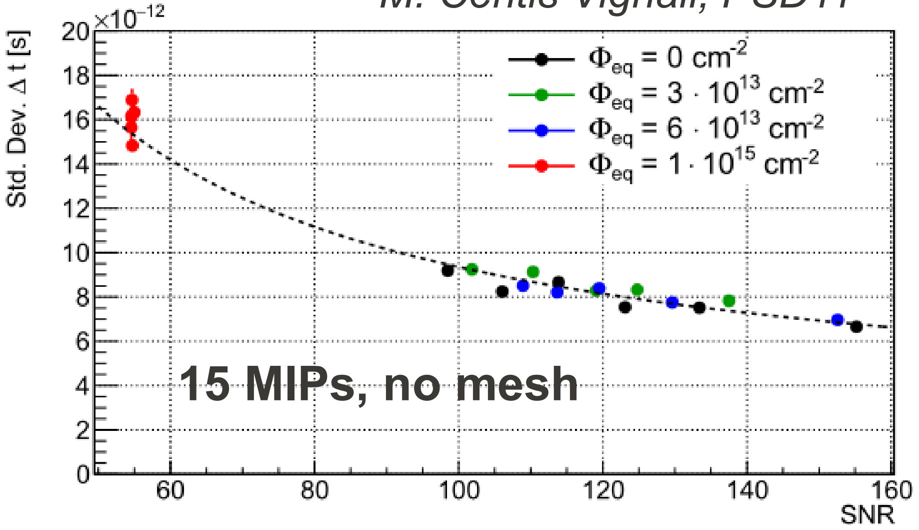

0: 1350-1475 V 3e13: 1425-1525 V
6e13:1500-1600 1e15: 1650-1750 V

Time resolution for **irradiated** devices vs SNR, for different fluences (irradiation with **neutrons**). Measurements with laser shining **~15 MiPS**.

Until 6×10^{13} n$_{eq}$/cm^2, gain decrease by irradiation, **compensated** by **raising bias**. For 1×10^{15} maximum maximum bias (1800V) reached without signs of gain.

Acceptor removal... with you since 1996

- **Deactivation** of acceptor **shallow** levels by radiation: **exponential depence on Φ**

- **Donor** and **acceptor** removal after *neutron irradiation* studied during LHC construction for 1-3 kΩ.cm, **n and p-type silicon**.
  - Removal **happens at low fluences** 10^{12}-10^{13} neq/cm^{-2}
  - Donor removal **depends** on **initial dopant concentration**
  - Measured **higher** removal rate **for donors** than acceptor (C_D=2.41×10^{-13}, C_A=2×10^{-13} cm^2)

NIMA 466 (**2001**) 308–326

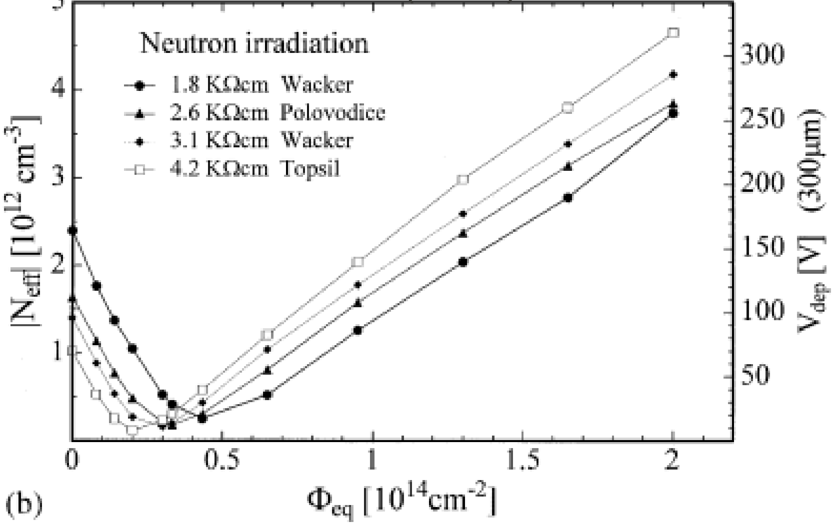

Donor removal → Acceptor introduction →

Higher initial dopant concentration leads to later "type" inversion and smaller Vdep

*NIMA 377 (**1996**) 228-233*

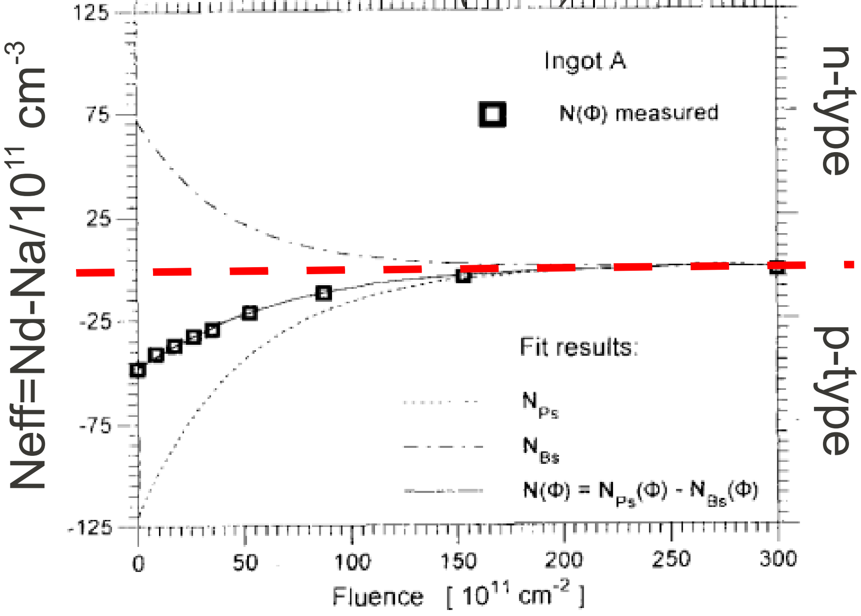

p-type material (compensated)
Simultaneous acceptor & donor removal

Acceptor removal

- **Lately**, acceptor removal with radiation has **gained focus** because of choice of **p-type** material for upgrades.

Acceptor removal shows a:

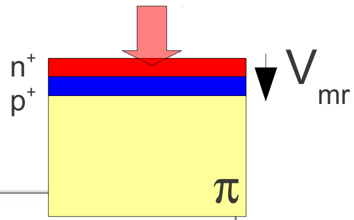

G. Kramberger, 24th RD50 Workshop, Bucharest, June 2014

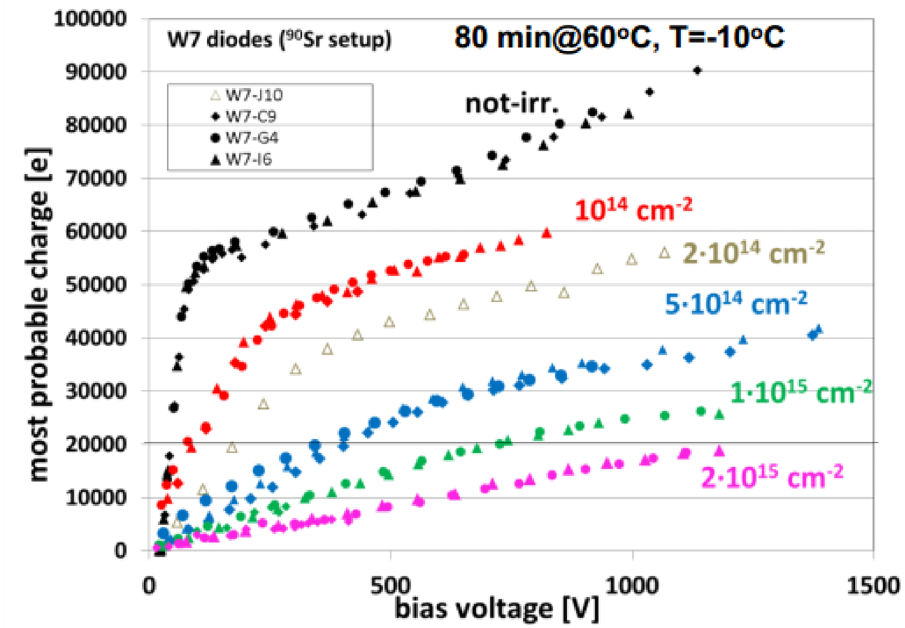

300 um PIN without multiplication

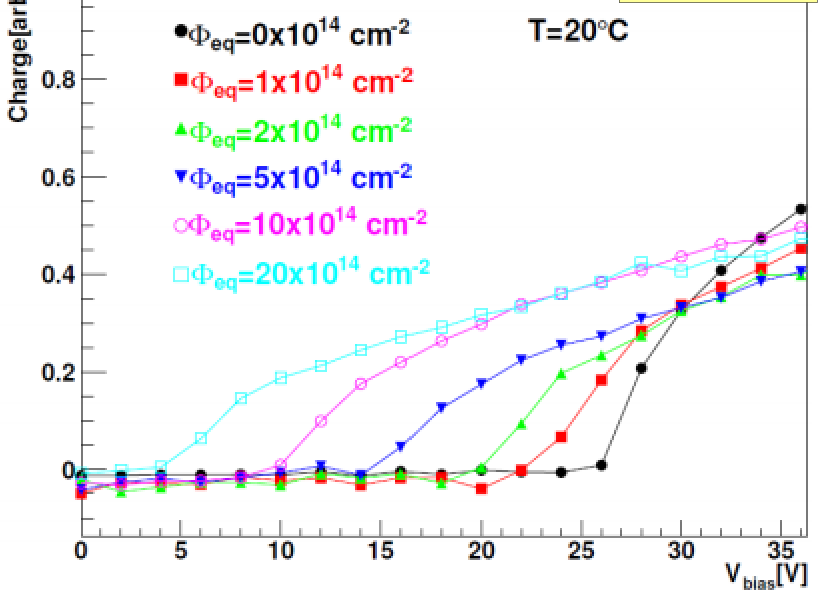

Detrimental effect for LGAD
Observed: loss of gain

Measured reduction of voltage needed to deplete multiplication layer.
Reason: reduced [B] concentration in multiplication layer.

See as well S.Ugobono's talk

Acceptor removal

- Lately, acceptor removal with radiation has **gained focus** because of choice of **p-type** material for upgrades.

Acceptor removal shows:

M. Fernandez, 27th RD50 meeting

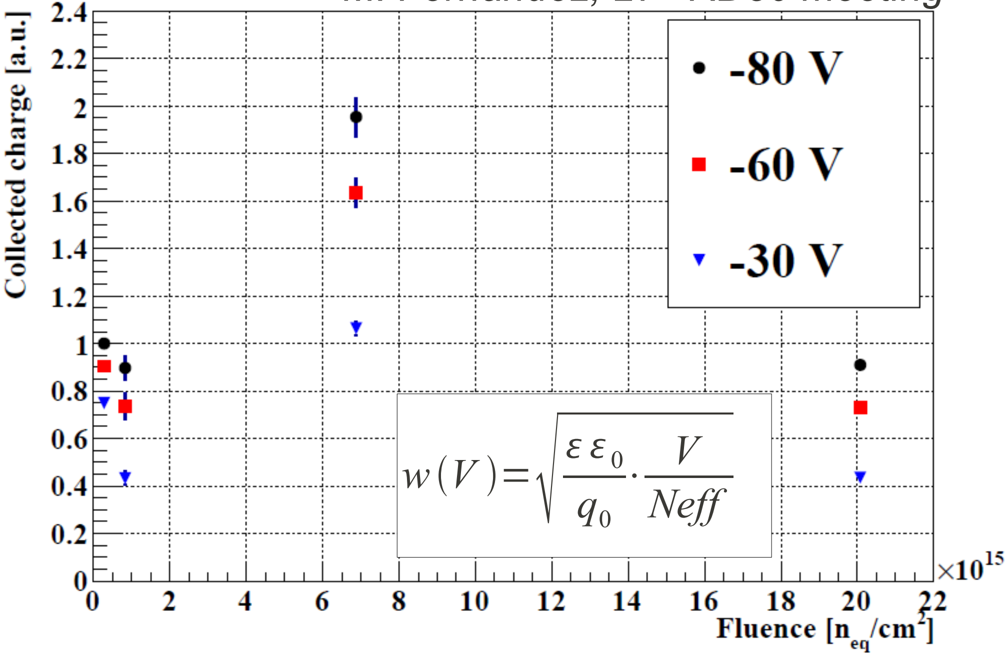

$$w(V)=\sqrt{\frac{\varepsilon\varepsilon_0}{q_0}\cdot\frac{V}{Neff}}$$

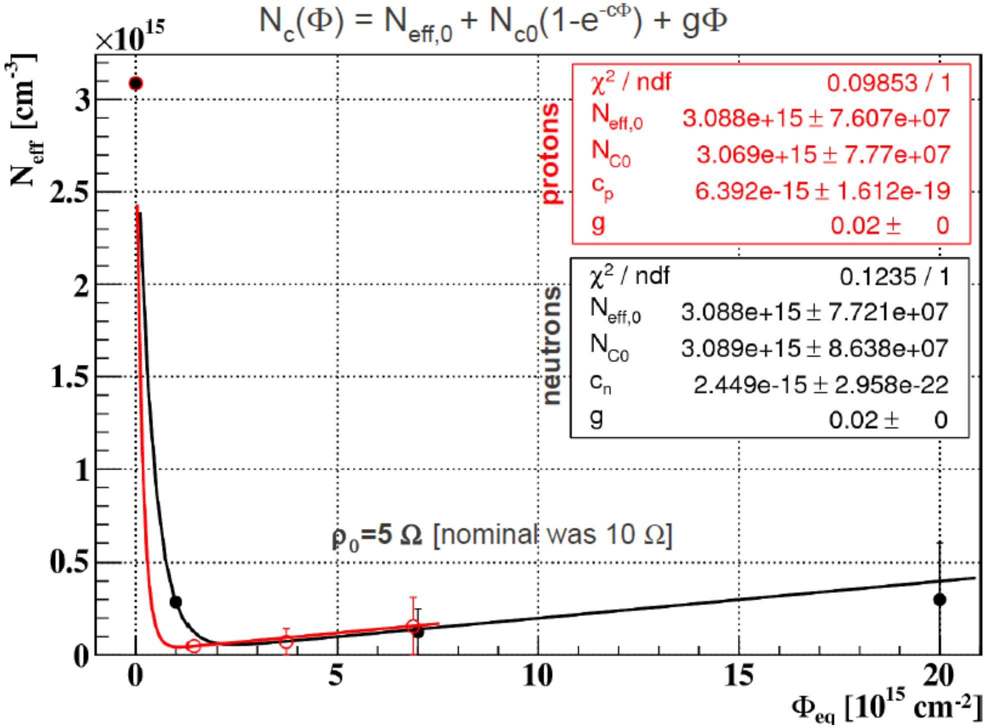

- **Beneficial effect** for low resistivity bulk of HVCMOS (CCPDv3, **10 Ω.cm**)
- **Observed:** Collected charge maximum at high fluence, then decreases by trapping.

- **Reason:** reduced dopant concentration in bulk → wider depletion region at same voltage

The fact that acceptor removal **is beneficial in low resistivity** bulk does not imply that the total collected charge is going to be higher than in High Resistivity-HVCMOS.
CC depends on resistivity, thickness and maximum voltage that can be applied.

Acceptor removal

- Within **RD50**, **systematic** study being conducted (**CiS campaign**) using a large number of identical sensors but varying thickness, doping and material type.

- Neutron (1e13-1e16) and proton irradiations (1e11-7e15) underway.
Sensor characterization:
  IV/CV analysis, TCT/edge-TCT, TSC
  Annealing studies after irradiation

- Thin epitaxial sensors**:** acc. **removal observed**

Results from electrical characterizations of proton and neutron irradiated devices agree with other recent results

$$N_{eff}(\Phi) = N_{eff,0} - \underbrace{N_C(1-\exp(-c\Phi))} + g_c\Phi$$

Higher removal constant "c" for **higher** resitivity materials. Removal will happen in the **first 10^{13}-10^{14} n_{eq}/cm^2**. In detectors with initial **lower resitivity**, **benefitial** effects are seen **at higher** fluence.

P. Dias de Almeida, 30th RD50

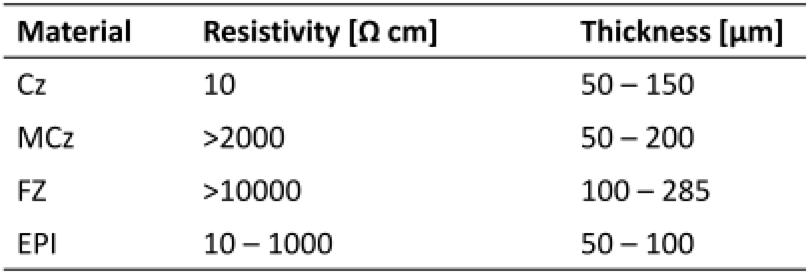

Material	Resistivity [Ω cm]	Thickness [µm]
Cz	10	50 – 150
MCz	>2000	50 – 200
FZ	>10000	100 – 285
EPI	10 – 1000	50 – 100

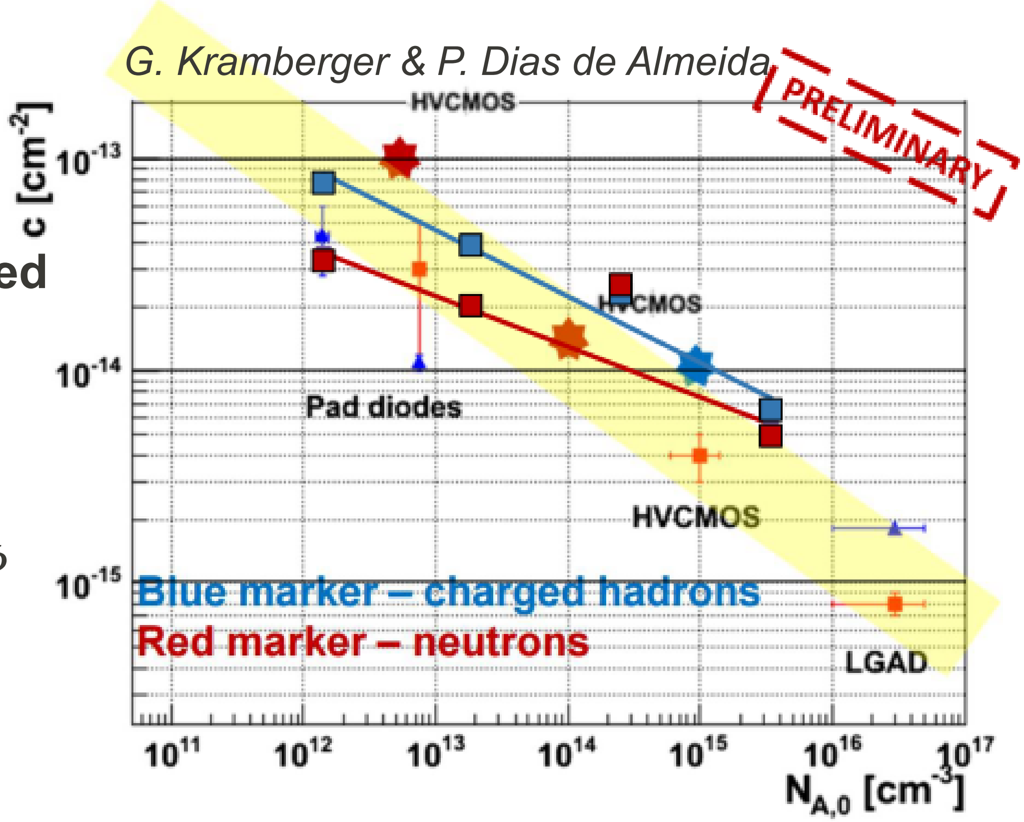

G. Kramberger & P. Dias de Almeida

Higher resitivity Lower resitivity

HVCMOS: material characterization

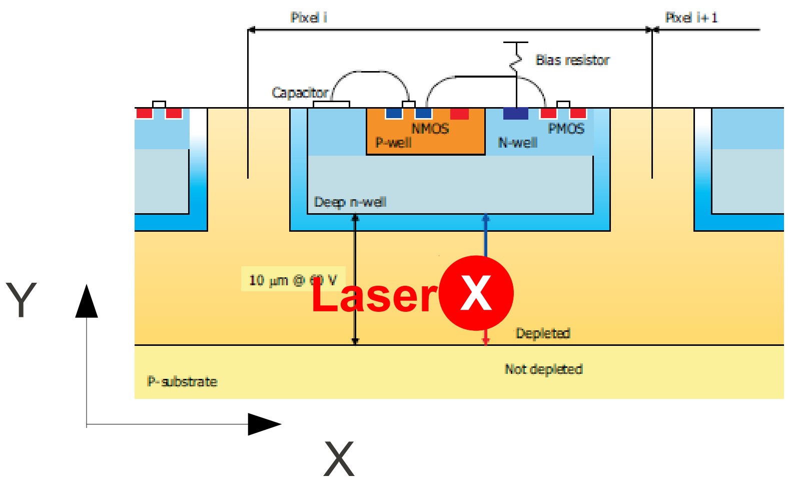

- **Material properties** of **different HV/HR-CMOS** coming **from different producers** are of **most interest** for RD50.

- When possible, **passive structures** (no nMOS/pMOS electronics) are measured directly. The current induced "at the DNW" is directly readout via a current amplifier.

- For an edge-TCT scan, raster scan in XY coordinates. Charge collection maps allow to identify the structure as a function of voltage too.

G. Kramberger 2016 JINST 11 P04007

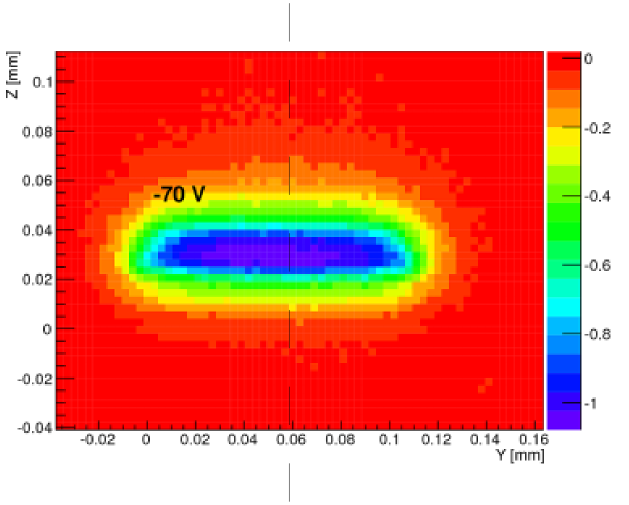

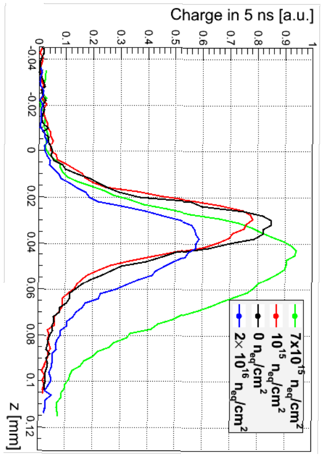

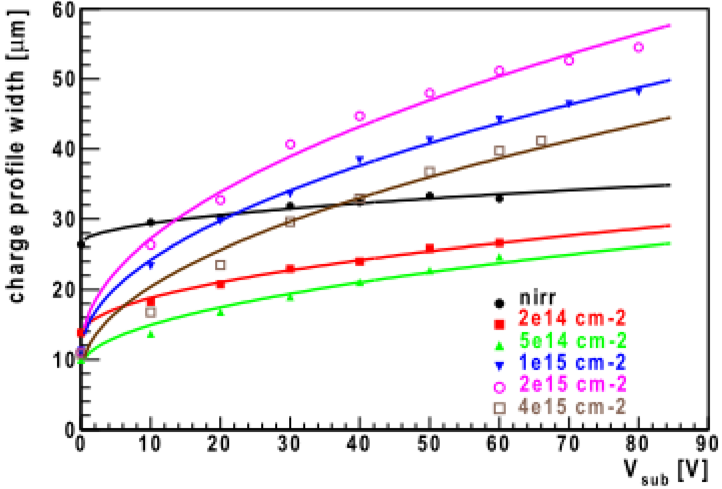

$$w(V)=\sqrt{\frac{2\,\varepsilon\,\varepsilon_0}{q}\,\frac{V_{bias}}{N_{eff}}}$$

HVCMOS: acceptor removal

- In the next 3 slides showing results of devices from 3 different foundries:

AMS (10,20 Ω.cm) → ATLAS CMOS **Strip** collaboration
X-FAB (100 Ω.cm), LFoundry (10-1000 Ω.cm) → ATLAS CMOS **pixel** collaboration

- Illustrating: acceptor removal, charge collection and front/backplane biasing

B. Hiti, Trento meeting 2017

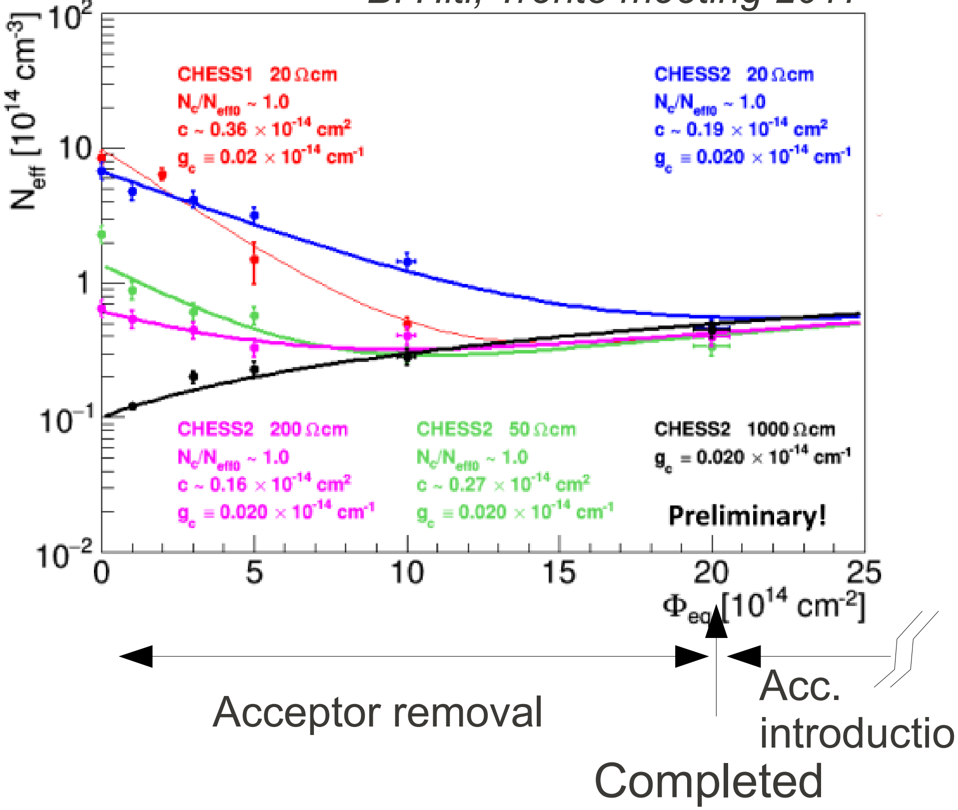

Acceptor removal

Acc. introduction

Completed

I. Mandic, 29th RD50 meeting

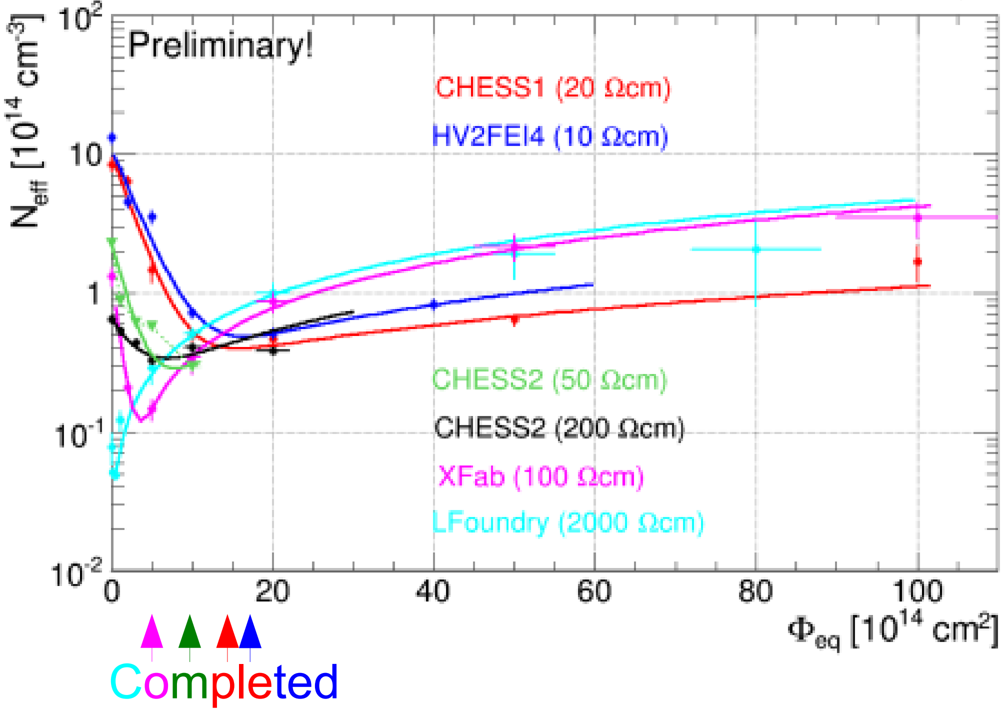

Completed

- Since the removal constant is not the same for all resistivities, the **point of complete removal** happens **at different fluences**. **From there on**, acceptor introduction is common to all devices and Neff(Φ) curves grow **parallel**.

HVCMOS: Charge Collection Efficiency

G. Kramberger 2016 JINST 11 P04007

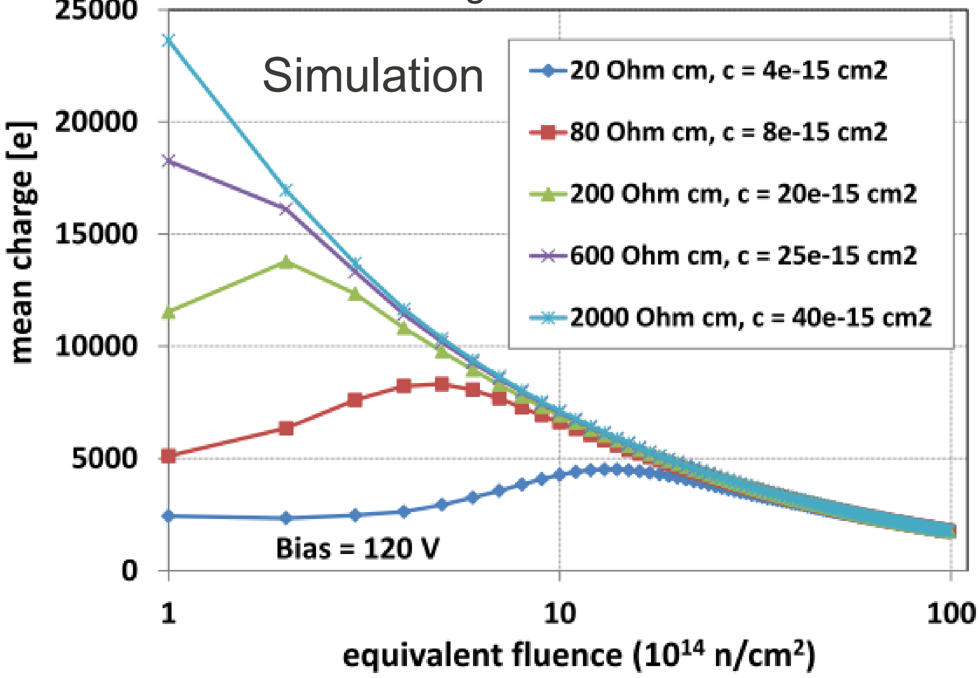

B. Hiti, Trento meeting 2017

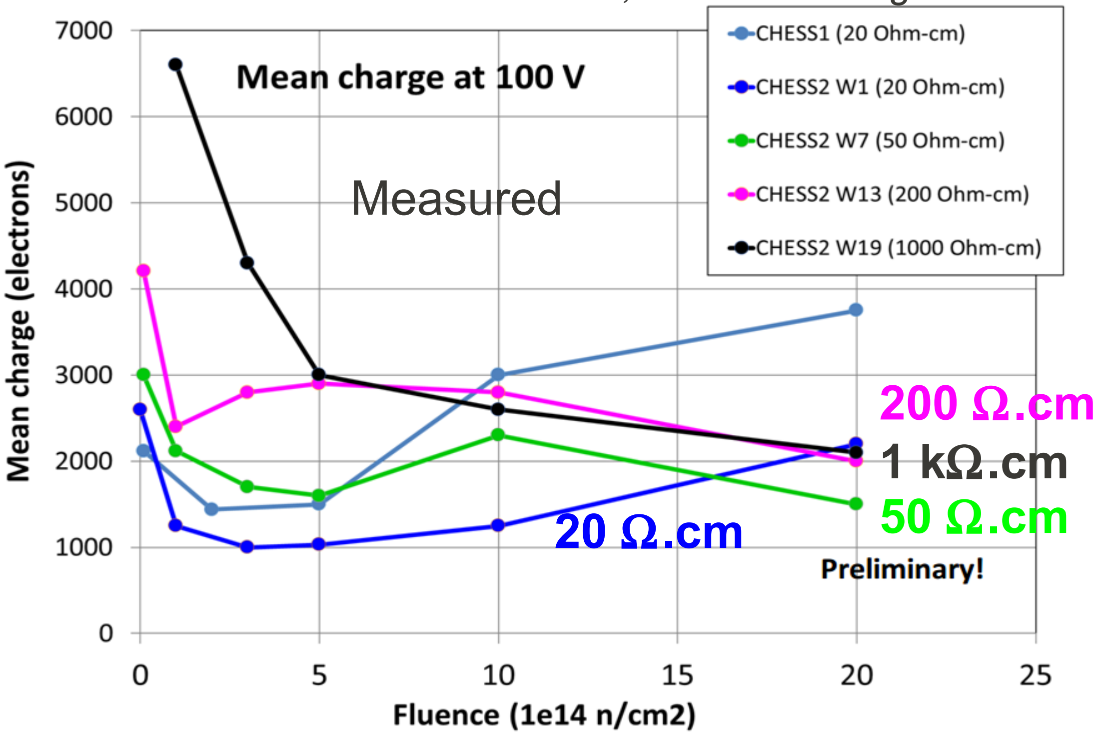

- Simple simulation of a large pad of HVCMOS detector of different substrate resitivities. In first order, CC expected to be very similar after donor removal (same Neff → same w(V) → same CC).

- Qualitative agreement to measurements of CHESS2 devices (AMS H35).
- **Higher resistivity favoured**: collects more at low fluences.

- Due to the interplay of Acc. Rem. and donor creation it seems **possible** to **find** a **resistivity** where **charge** is **not degraded** for the **full fluence range**

HVCMOS: front versus back biasing

I. Mandic, 30th RD50 meeting

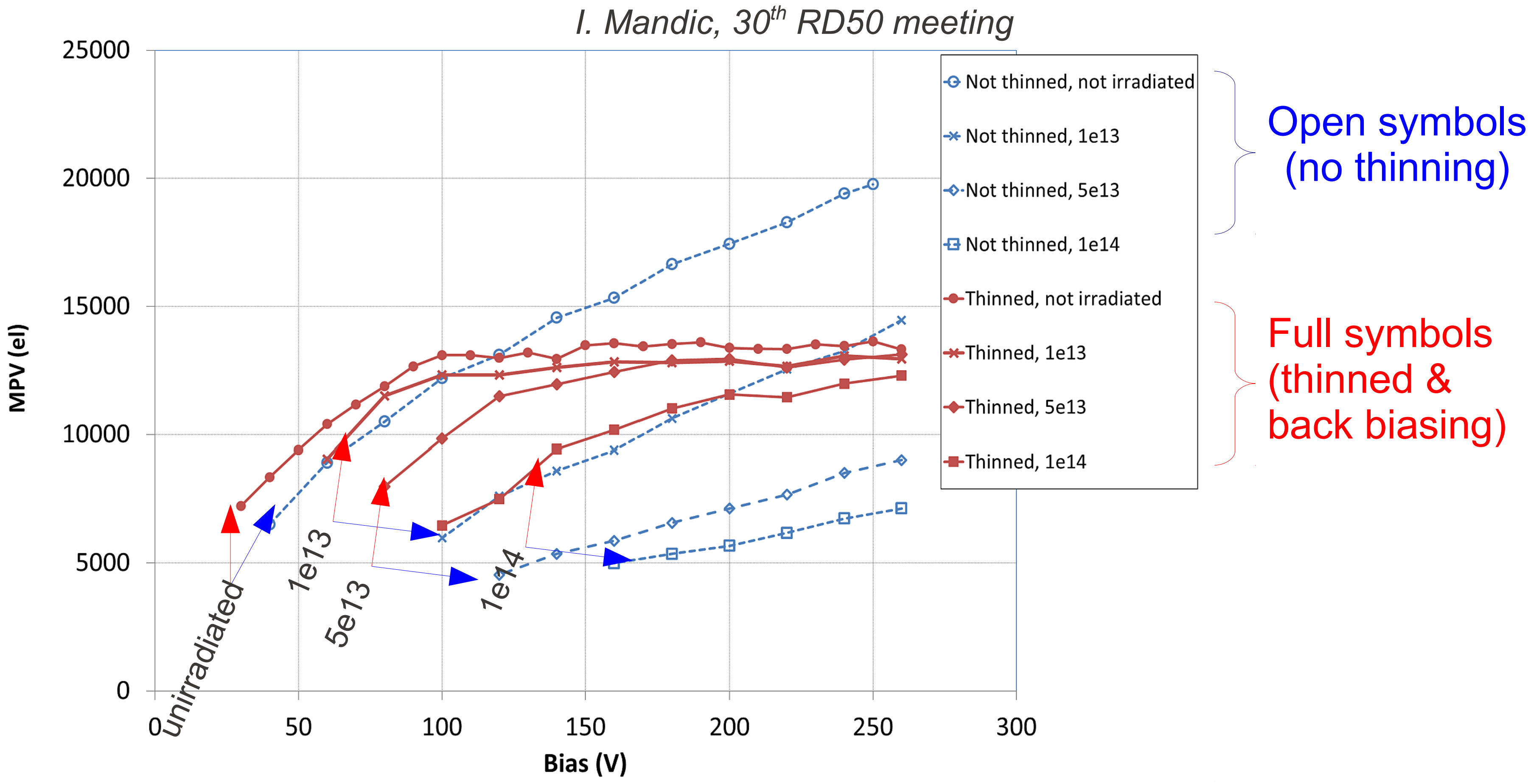

Open symbols (no thinning)

Full symbols (thinned & back biasing)

ATLAS LFoundry demonstrator: 150 nm HR-CMOS (>2 kΩ.cm), V_{BD}=175-400 V

Higher collected charge (using Sr90 source + CSA 25 ns integration) measured for **backside bias & thinned detector** versus thick sensor (same active thickness) & front biasing.

RD50 HV-CMOS submission in LFoundry 150 nm

RD50 submission chip to LFoundry.

Goals: Improve timing resolution of HVCMOS sensors, new sensor cross sections and stitching options

Three timing matrices:

Matrix 1: Time stamp determination via sampling of raising edge

Matrix 2: In pixel-TDC for leading and trailing edge capture

Matrix 3: Very fast amplifier to recover BL voltage after < 2 Bxs

Matrix 4: new sensor cross section
Matrix 5: pre-stitching options (increase the device area beyond the reticle size limitation).

+ Test structures:
For instance for optical TCT/e-TCT measurements

E. Vilella, 30th RD50 workshop

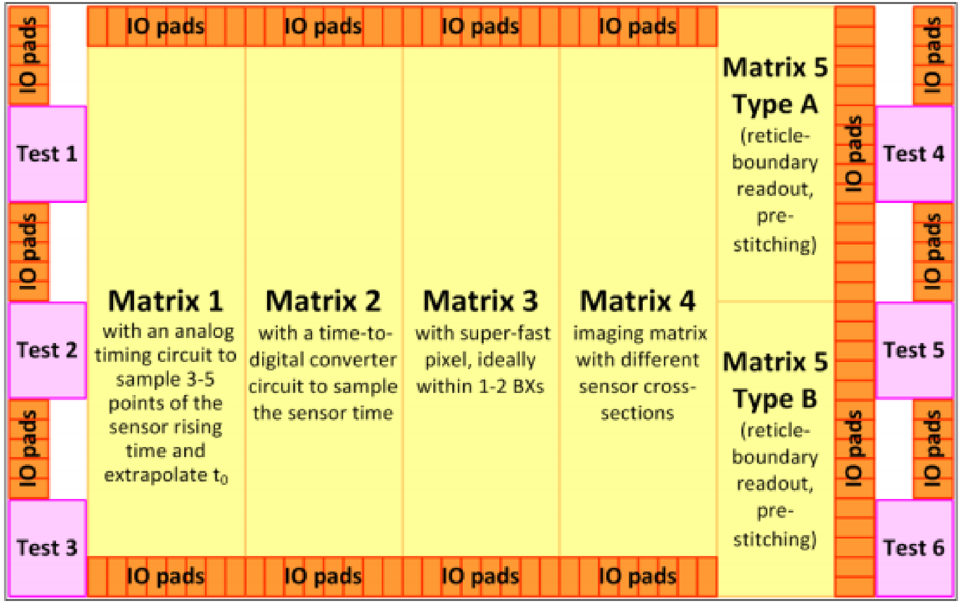

Lfoundry features: <120 V, ρ~10-4k Ω.cm (<=170 µm), Quadruple PN wells, backside biasing & stitching

MPW **to be sent** by next submission round: **November 2017**

Summary

Activity in RD50 organized around several workgroups including, defect studies, new sensor technologies, TCAD and fast simulators, new characterization techniques,...

Close link to R&D foundries (CNM-IMB Barcelona, FBK- Trento) **and commercial** companies (CIS, Micron,...) allow for fast and efficient development of new sensor concepts.

RD50 keeps **close links to the LHC experiments**. Most of groups in RD50 are part of ATLAS, CMS or LHCb.

Some **hot**-topics are actively studied in RD50: **acceptor removal**, detectors with **gain**, **timing** in Silicon, to mention some.

RD50 co-funds “common projects” involving several RD50 institutes targeting a specific R&D question (thin LGADs, 3D for HL-LHC, Ga doping of LGAD, TPA-TCT, RD50 common Test Beam, RD50 CMOS submission).

Some of the **most important** contributions **triggered by RD50** collaboration towards the upgrade of LHC: *p-type silicon, double column 3D detectors, radiation damage models for TCAD simulations, radiation damage models for experiments operation, fast timing in Si, new characterization techniques...*

NEXT CHALLENGE: The **FCC**

28th RD50 meeting Torino (2016)

Coffee break

30th RD50 meeting Krakow (2017)

RD50

+ information

Workgroup 2: development of new measuring techniques

edge-TCT

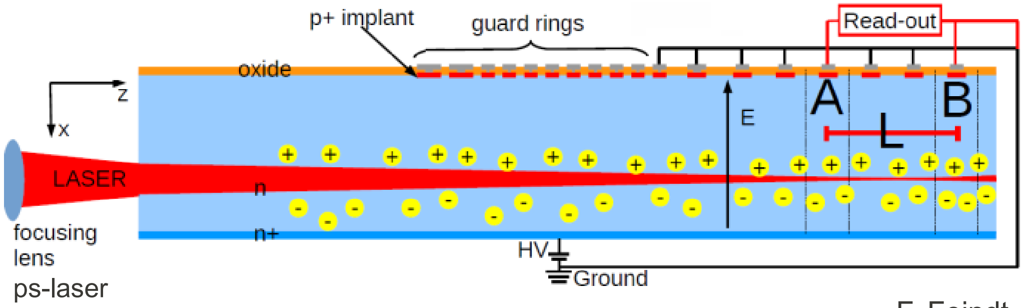

F. Feindt

TCT (Transient Current Technique): resolves movement of carriers and gives information on the electric field of the detector.

In **edge-TCT** (G. Kramberger et al) an IR beam is injected from the side of the detector. Detector can be probed as a function of depth. Continous carrier trail along beam.

G. Kramberger 2014 JINST 9 P10016

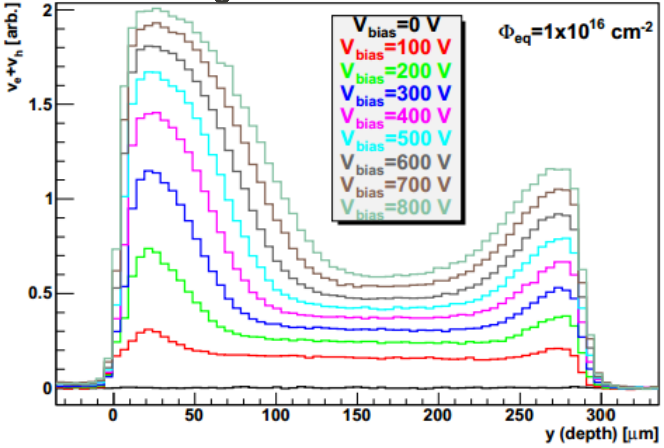

TPA-TCT

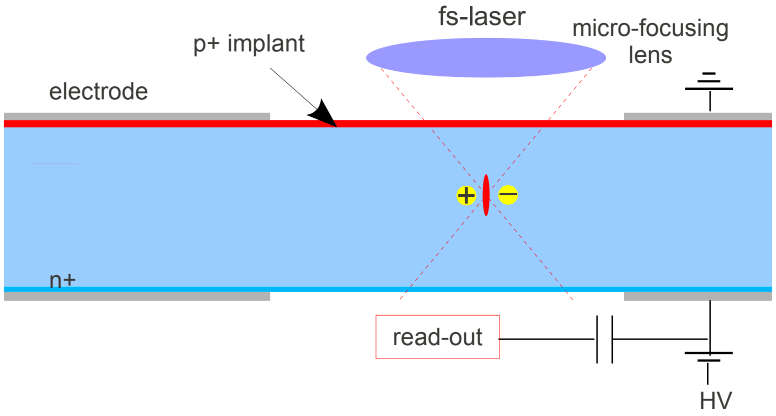

TPA(**Two Photon** Absorption)-TCT provides a **"point-like"** carrier generation volume: 3D spatial resolution

It uses strong microfocusing of a **sub-bandgap** laser to excite **non-linear** effects in Si.

M.Fernandez, NIM A 845 (2017) 69–71

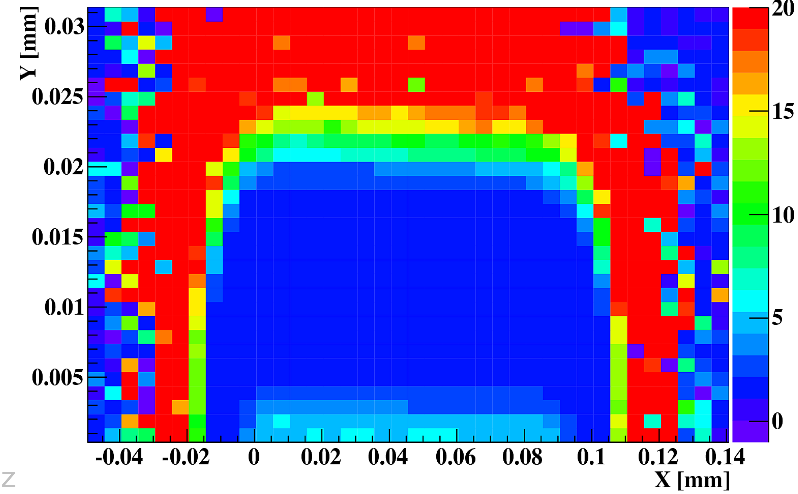

Acceptor removal mitigation tests
Ga-doped and C-sprayed LGADs

Radiation hardness of Ga-doped LGAD

G. Pellegrini, 30th RD50 meeting, Krakow
G. Kramberger, 30th RD50 meeting, Krakow

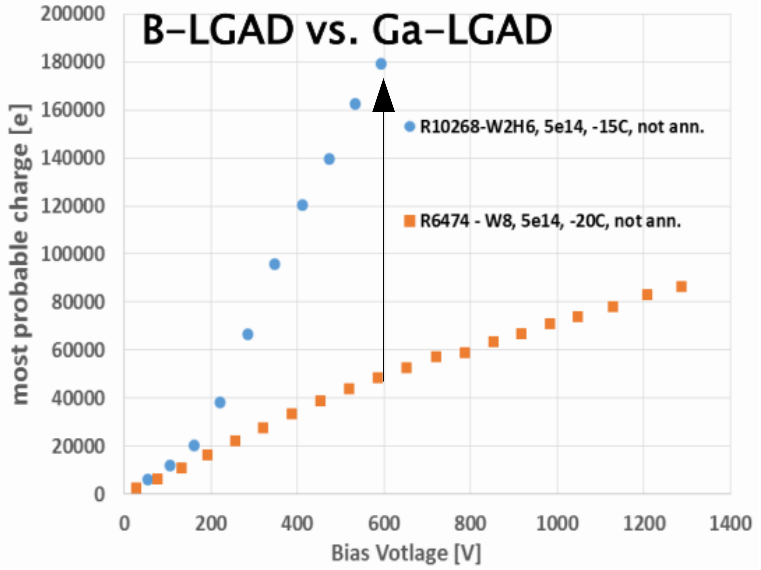

CNM run 10628, with 4 different gains, 285 um thick. Premature break before multiplication layer has been depleted. But once they are irradiated, devices work!

Up to **x3 increase** of **collected charge** with Ga-doped **after 5e14** and **1e15**, compared to “standard” B-doped LGADs. Up to **x2 for 2e15**

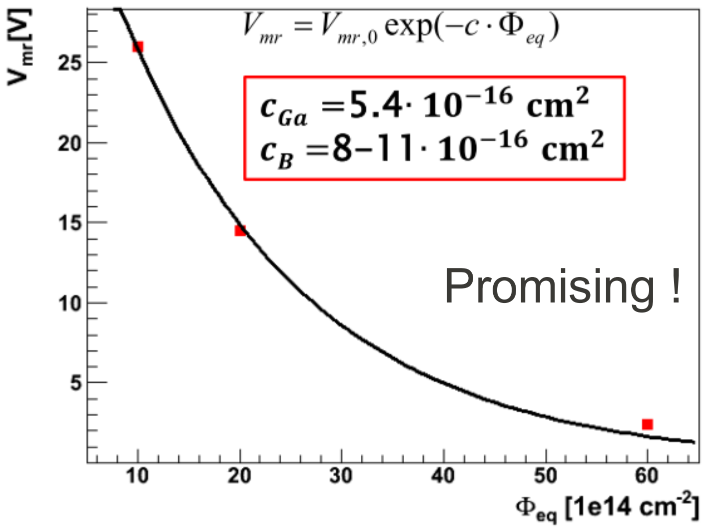

Promising !

Smaller removal constant – about twice smaller than in B doped devices

Production of **thin** Ga-LGADs as RD50 project

LGADs with C-spray

G. Pellegrini, 30th RD50 meeting, Krakow
G. Kramberger, 30th RD50 meeting, Krakow

CNM run 9889

B and C compete for interstitials
Less I's available → lower probability of B-removal by:
I + Bs → Bi ; Bi + Oi → BiOi

Ga-LGAD , C-spray LGAD, B-LGAD

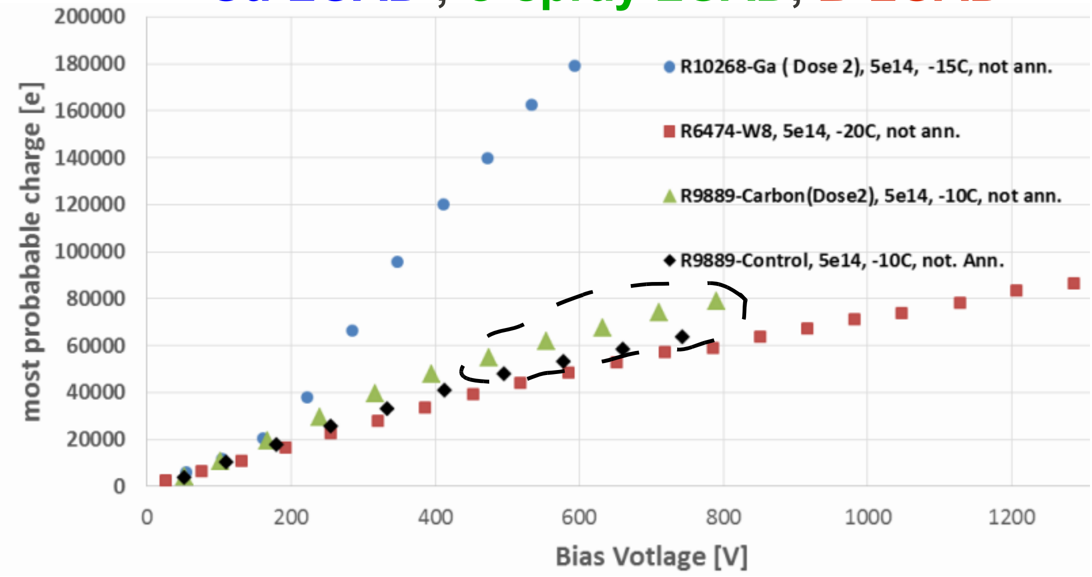

Improvement is small ~20% but this may depend on the concentration of sprayed C in B implant

300 µm high resistivity p-type wafers

Carbon can reduce the Boron and Phosphorus diffusion. Because of that variation, 5 Pwell imp. doses have been used

Study of new ATLAS pixel implantations

Six modified IBL (FEI4) pixel designs investigated. Identified one with best performance in terms of MPV/ToT, efficiency at lower voltages and up to 5e15 neq/cm2.
Slightly higher leakage current for the new design

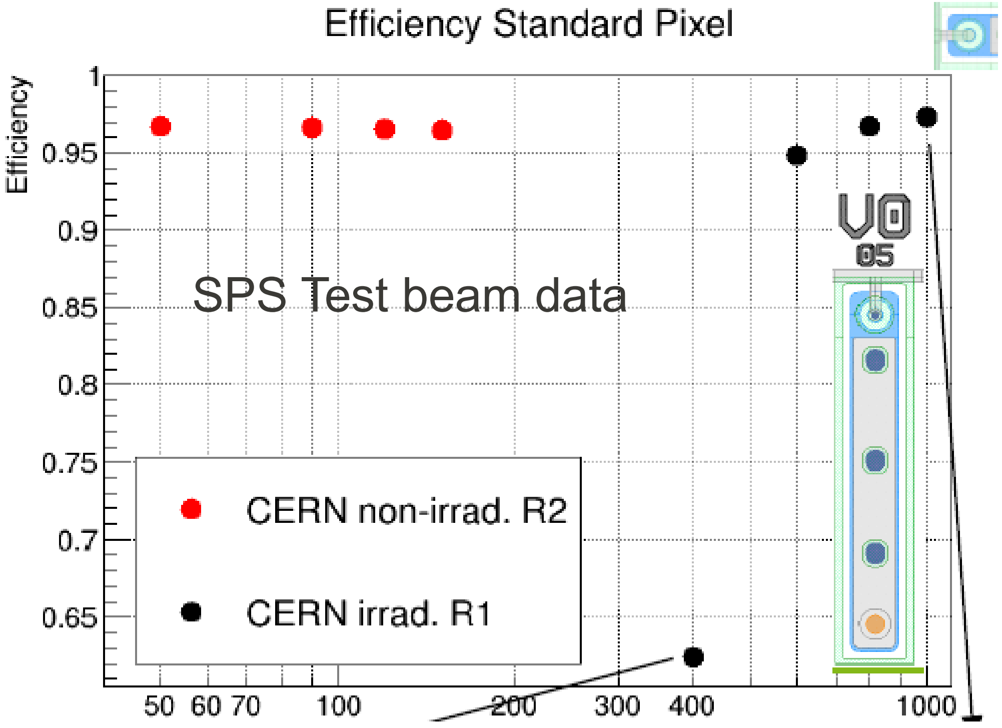

A. Gisen, 30th RD50 workshop

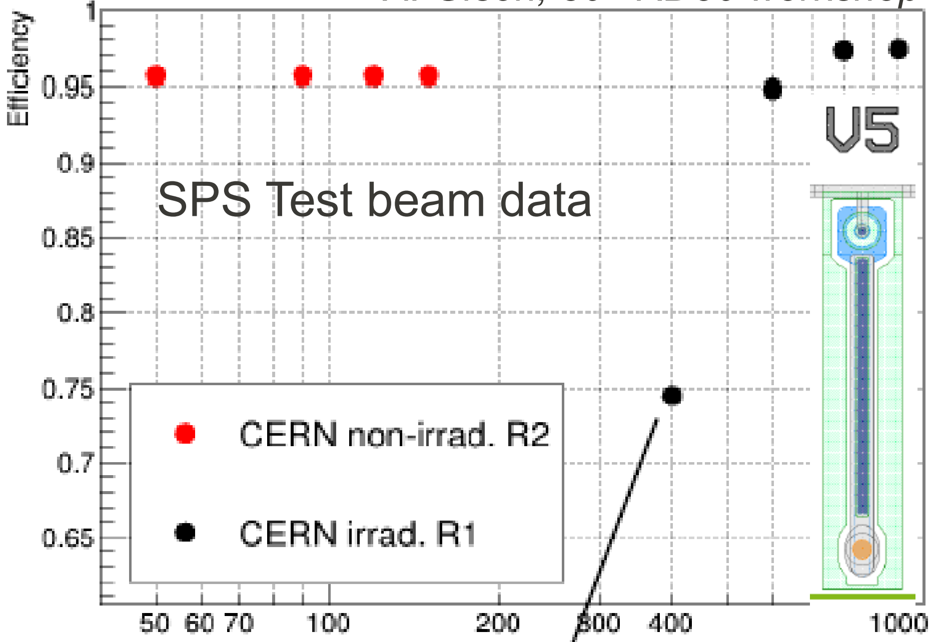

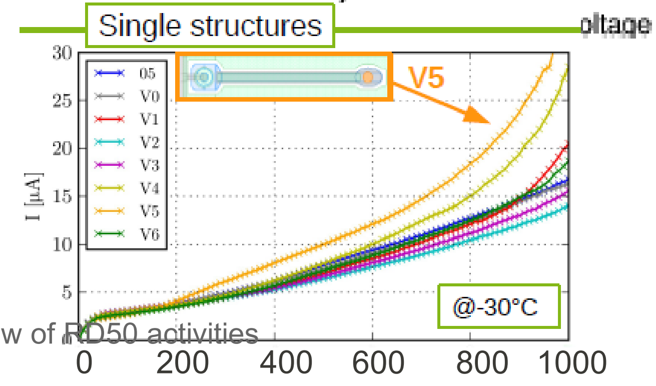

New production, based on v5 with some modifications expected by mid-October 2017.

Radiation hardness of 3D detectors

3D and planar for ATLAS pixel upgrade

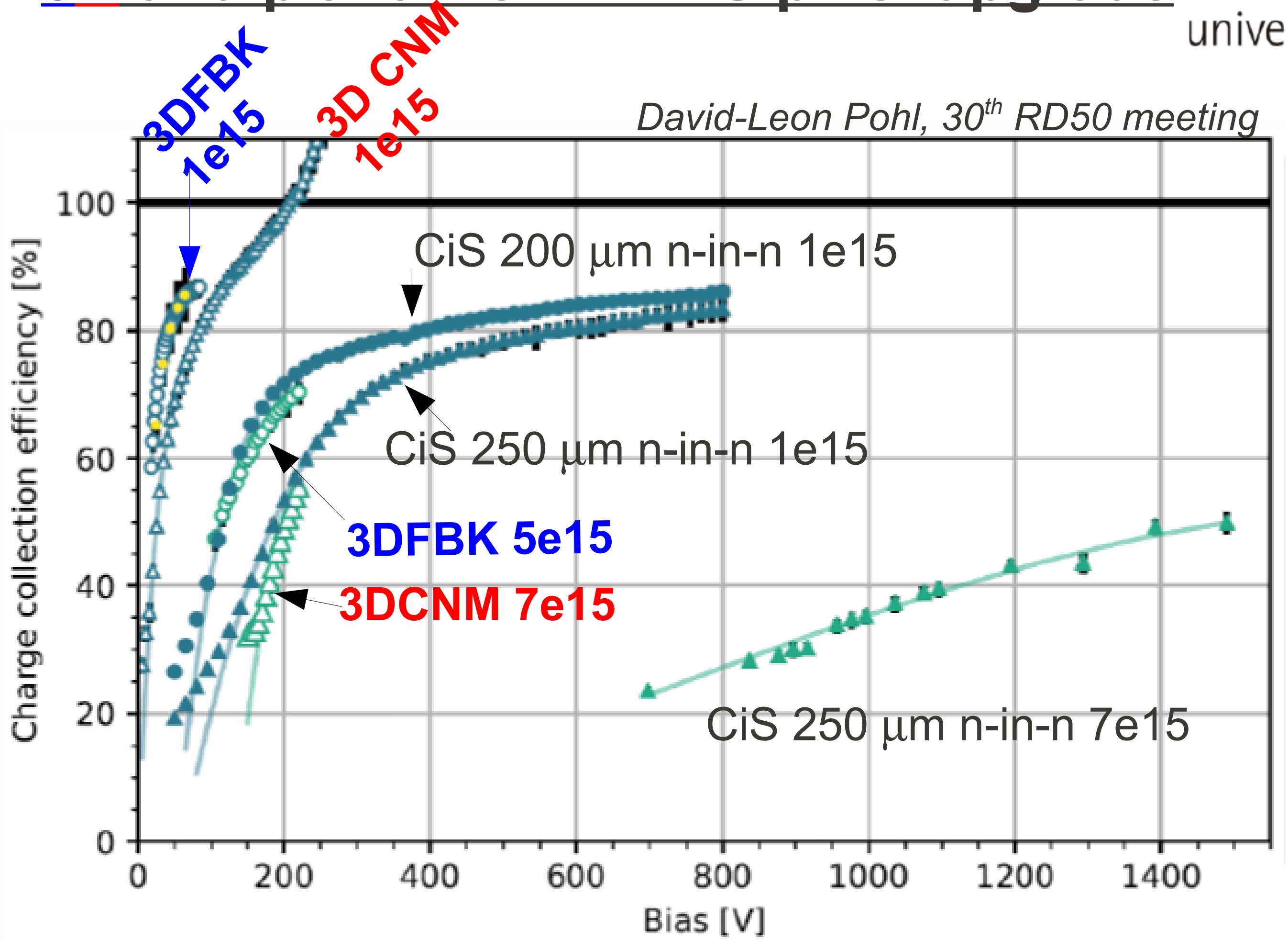

Full symbols, CiS planar, n-on-n
Open symbols: 3D, n-on-p
Lines: simulations
Detectors from IBL production
[Fluences in n_{eq}/cm^2]

Using ATLAS FE-I4, Sr90, 24 MeV protons
CCE(200 µm,planar)>CCE(250 µm, planar)
7e15: 50 % CCE reached for planar at >1400 V
50 % CCE reached for 3D at 200 V

Special effort done in comparing data with **simulations**. New open-tools developed:

SourceSim for RS simulations
SCARCE: for CCE studies

Some parameters (Neff,trapping) obtained from fits of simulation to data

Passive CMOS for ATLAS pixel upgrade

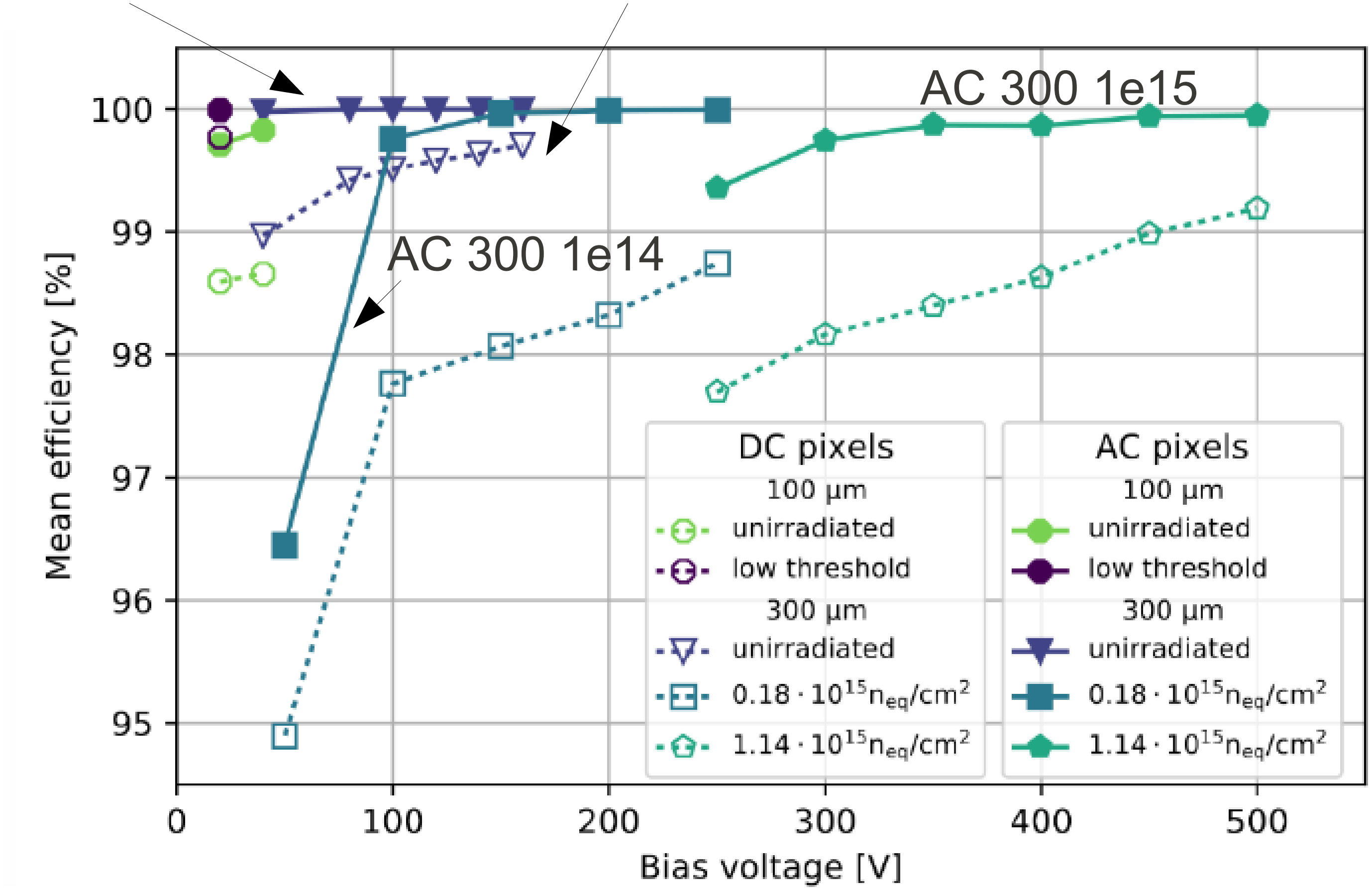

AC 300 non-irradiated

DC 300 non-irradiated

AC 300 1e15

AC 300 1e14

Rounded open: DC 100 µm
Not open DC: 300 µm
Rounded full AC: 100 µm
Remaining full AC: 300 µm

LFoundry 150 nm CMOS, 4 kΩ.cm, 100/300 µm
AC coupling improves efficiency due to missing bias dot
Efficiency=99.97 AC pixels, 99.2% DC pixels

Radiation hardness of small-pitch 3D pixel sensors up to HL-LHC fluences, J. Lange

Radiation hardness of 3D pixel sensors with small pixel sizes of 50x50 (this work) and 25x100 µm² (Esteban) produced by CNM Barcelona (run 7781, RD50) tested up to HL-LHC fluences

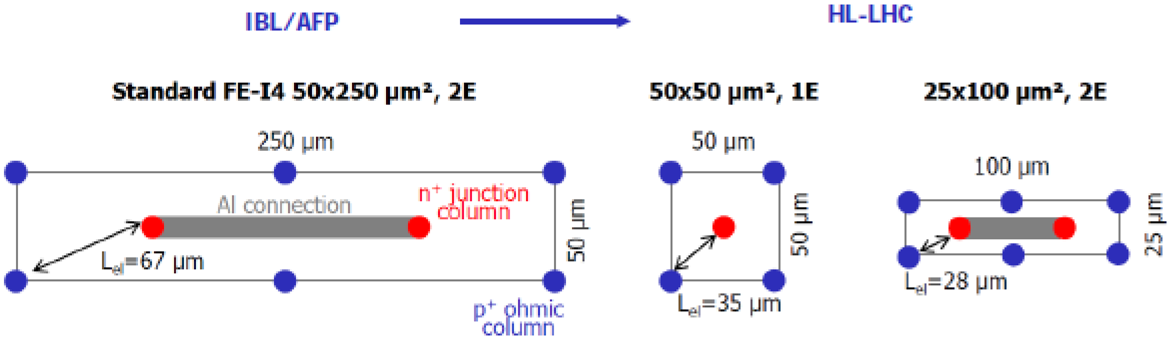

Proton irradiation campaigns:

1) KIT, uniform, 23 MeV, 5e15 n_{eq} /cm^2

2) CERN-PS, non-uniform, 23 GeV p, 1.4e16 n_{eq} /cm^2

Benchmark efficiency of 97% reached at lower bias voltages than IBL sensors:

40 V at 5e15 neq /cm2 (-25◦ C)
100 V at 1.4e16 neq /cm2 (-25◦ C)

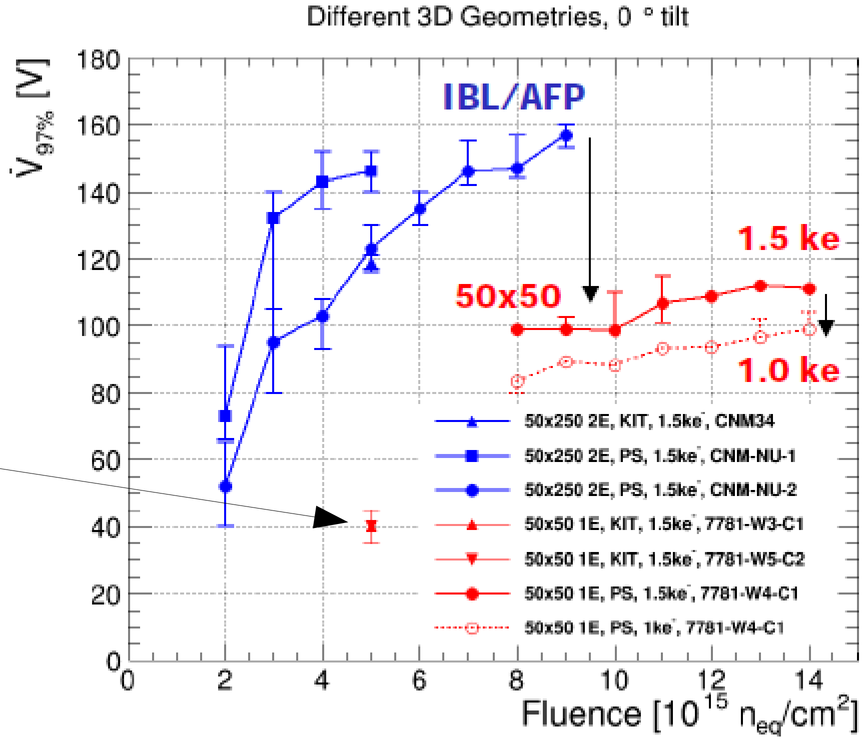

Power dissipation can be kept at low levels of 1.5 mW/cm² at 5e15 neq /cm2 (40 V, 97 % eff, -25 C) and 13 mW/cm² at 1.4e16 neq /cm2 (100 V, 97%eff, -25◦ C)

Characterization of small-pitch 3D sensors from CNM
E. Curras

Instituto de Física de Cantabria

Centro Nacional de Microelectrónica CSIC

RS and TB measurements of 3D sensors (50x50 and 25x100 cell size, 1E configuration) in strip configuration readout by Alibava. Run 7781, RD50 run, same as IFAE

Unirradiated Vdep~5V. Here, 15 ke at 0V!

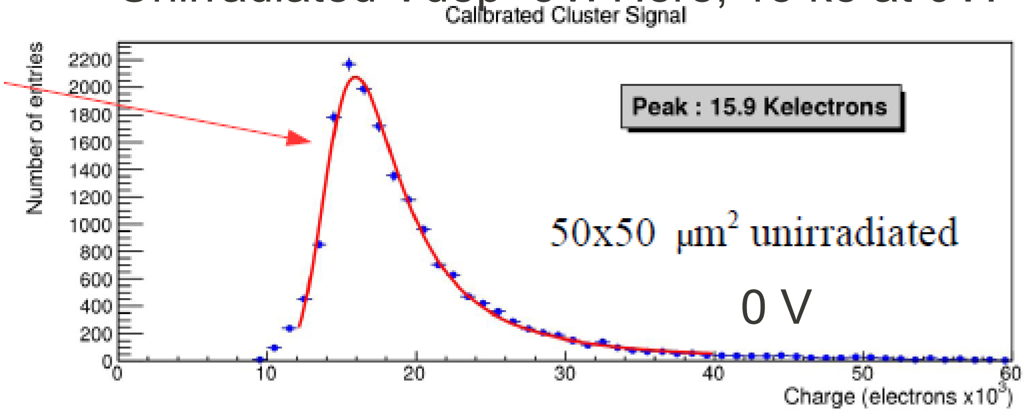

Proton irradiation SPS

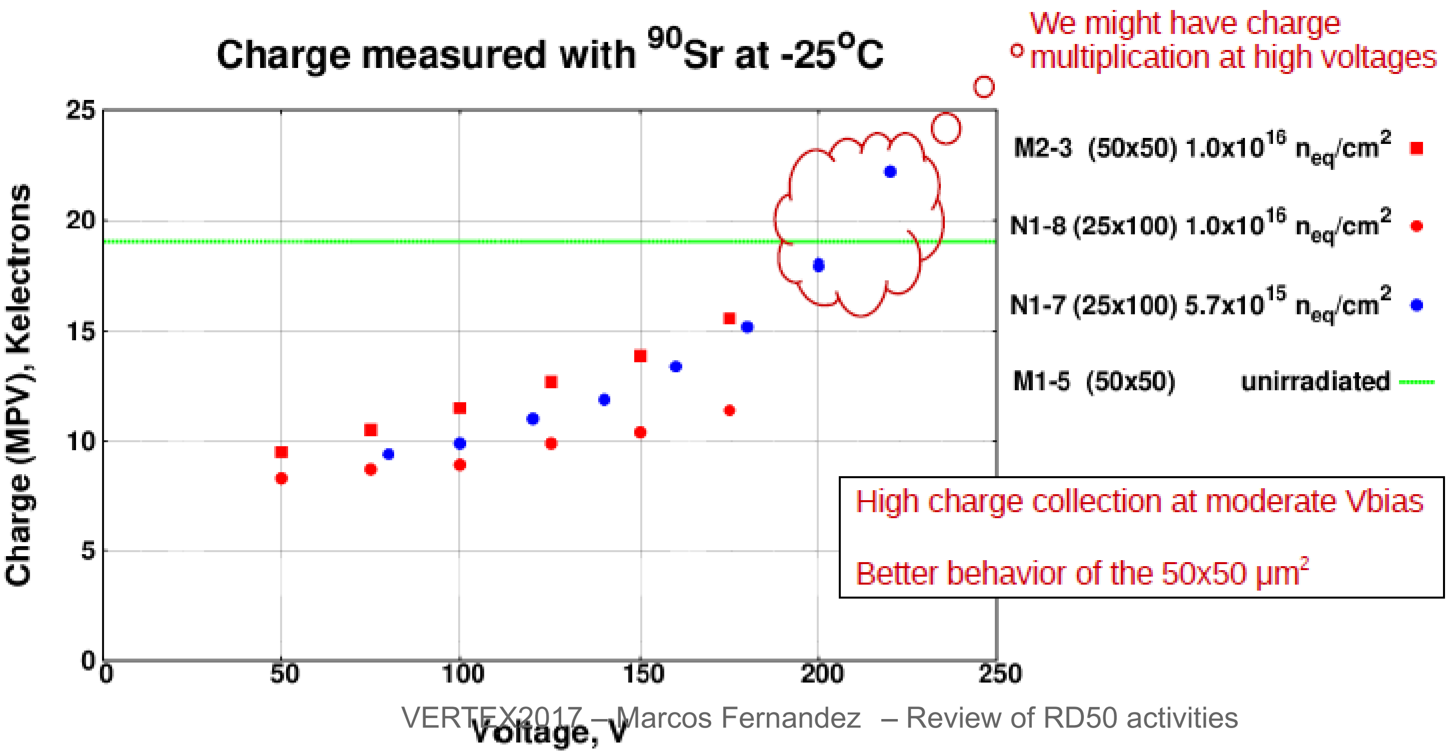

We might have charge multiplication at high voltages

High charge collection at moderate Vbias

Better behavior of the 50x50 µm^2

Measurements of Irradiated 3D Strips Sensors

Run 7781, 3D Double Side Process, 230um thin wafers, neutron irradiation in Lbj

3D in strip configuration: all 1E, 50x50,25x100,30x100

Strip	Pixel cell size (μm^2)	L_{el} (μm)
7781-8-M2	50x50 1E	35
7781-4-O	30x100 1E	52
7781-4-M1	50x50 1E	35
7781-4-N1	25x100 1E	51
7781-4-M2	50x50 1E	35

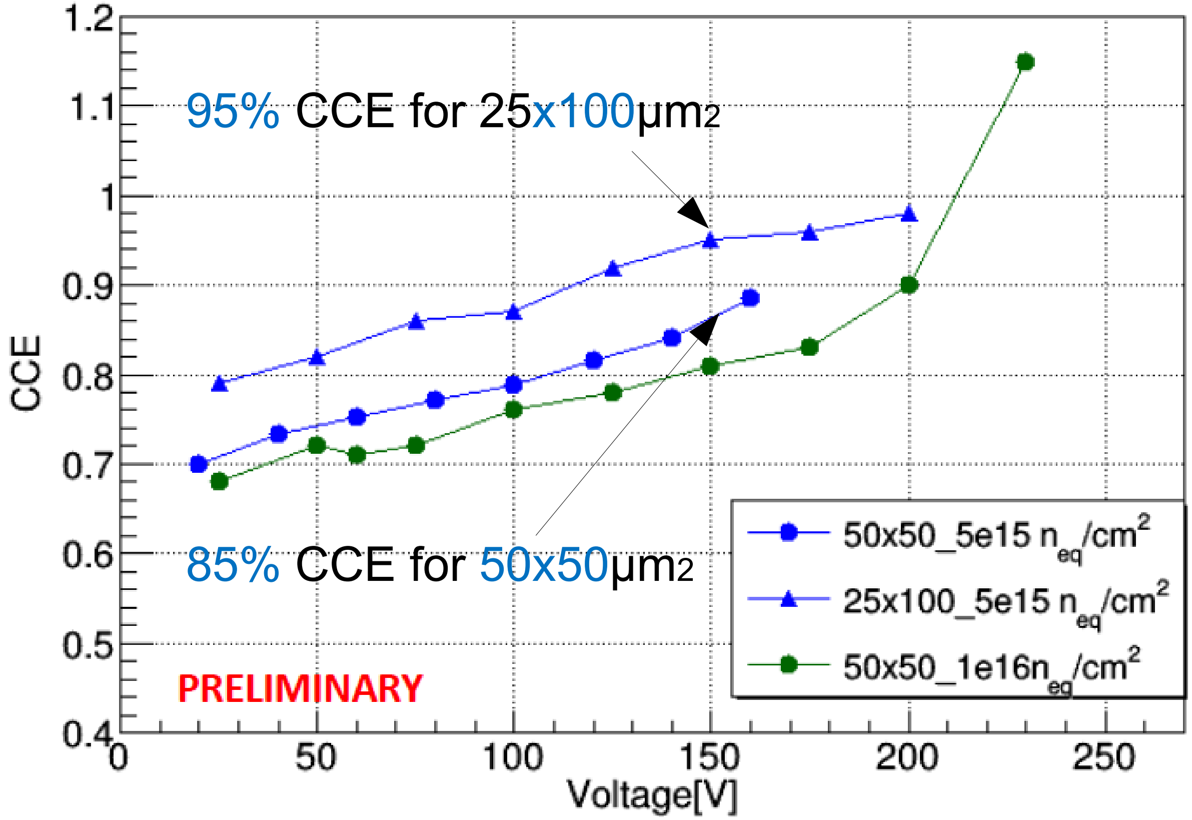

95% CCE for 25x100μm$_2$

85% CCE for 50x50μm$_2$

PRELIMINARY

Higher CCE for 25x100 despite higher collection distance!

At 220V, 100% CCE achieved by 50x50μm$_2$, 1e16 n$_{eq}$cm$_{-2}$

Acceptor removal

Interpretations of the observed acceptor removal effect

1) the measured changes are all due to a physical removal process of the shallow dopants. Interpretation backed up by continuous light illumination of LGAD devices (constant T). Changing a lot the SC (all DLs filled) does not change the gain.
See for instance: G. Kramberger, 28th RD50 Torino

2) TCAD simulations by R.Palomo (11 Trento workshop) and R. Dalal (NIMA A 836 (2016) 113–121) show qualitative agreement of calculated CCE(V) for different fluences.
Gain degradation can be explained by TCAD effective Deep Levels

3) **Quantitive** agreement (Ioffe's Institute, 2016 JINST 11 P12012) needs some externally removed acceptors to describe CCE measurements.

Note: no TCAD simulation available yet to explain measurements described in “1)”

R. Wunstorf et al, NIMA 377 (1996) 228.)
J. Adey, PhD Thesis, Univeristy of Exceter, 2004
J. Adey et al., Physica B 340–342 (2003) 505–508

Acceptor removal

$$dN_A = -\sum_i c_i \cdot N_A \, d\Phi \quad , \quad c = \sum_i c_i([O],\overset{?}{[C]},[B])$$

Radiation produces V and I – their spatial distribution depends on irradiation particle (large concentration of V,I in the cluster but small supply of [B] in the cluster)

Vacancy channel : V + Bs → VB (complex anneals out at T~0°C - no role)
Interstitial channel : I + Bs → Bi (dominant channel for B removal)

B_i = highly reactive ⇒ Can form different complexes with impurities resulting in:

- Acceptors in lower part of the band gap (negative space charge- BiBsH) – <u>incomplete removal</u>
- Donors in upper part of the band gap (positive space charge – BiOi) – <u>larger effective removal rate</u>
- Electrically inactive defects

Carbon rich environment: I + Cs → Ci competing reaction (smaller removal rate)

Oxygen rich environment: apart from forming complexes plays role in enhancing/reducing the concurrent reaction channels:
(e.g. V+O->VO instead of V+I->Si_s leaving more interstitials available)

2013 JINST 8 P08002

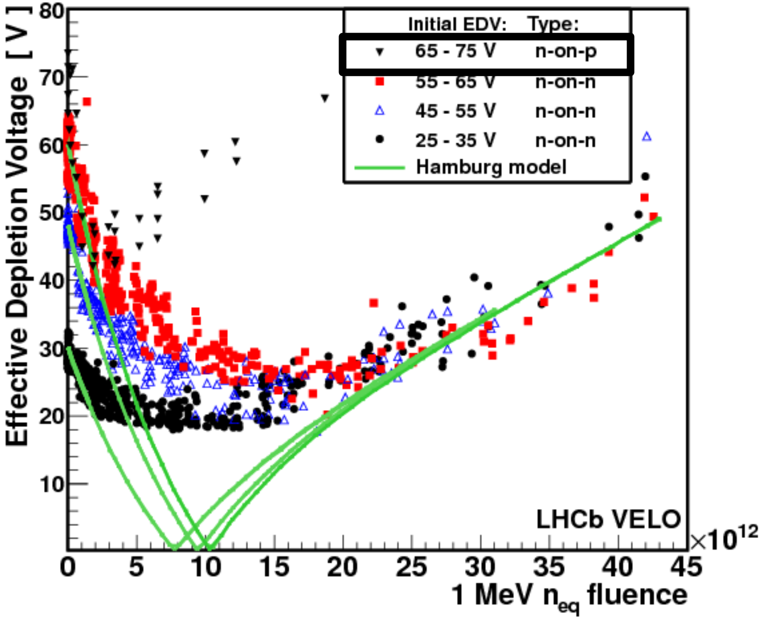

Initial depletion voltage decrease of ~25 V, then increases as the n-type

Leakage Current and Depletion Voltage Simulation for the ATLAS Pixel Detector, J. Beyer MPI

Using Hamburg model (parameters extracted from fit to ATLAS data) to predict different depletion voltage scenarios of ATLAS pixel after LS2

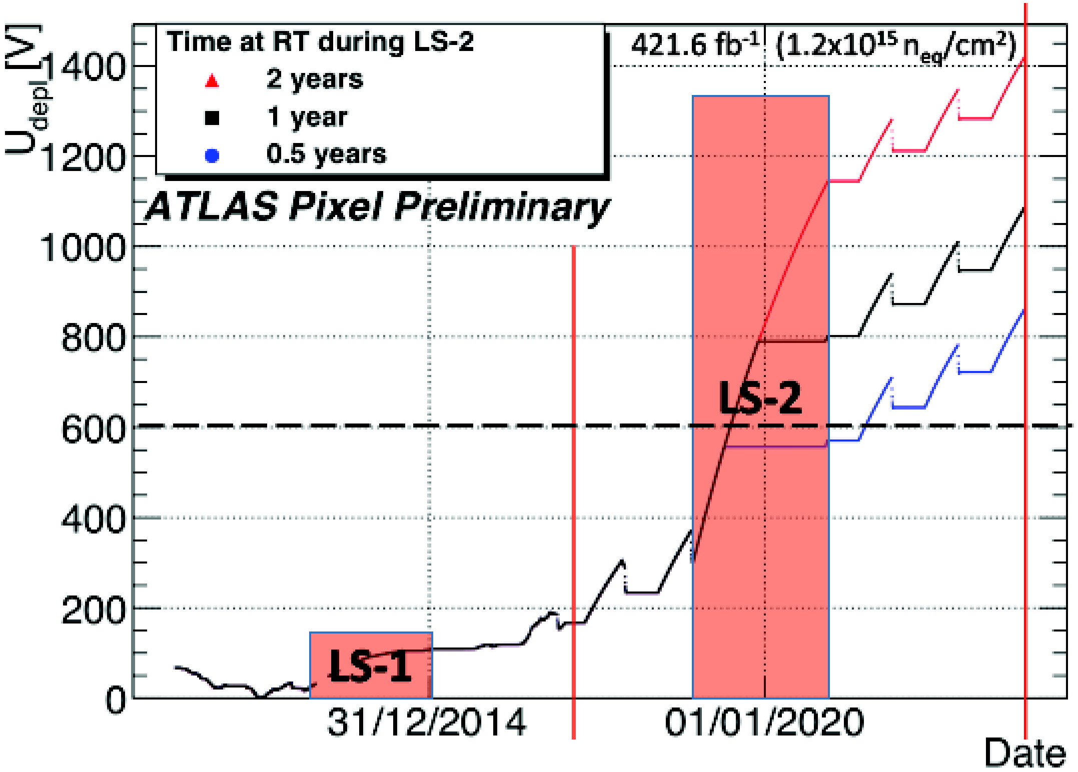

B-layer currently at Vdep=200 V
Plot above compares Vdep predictions for different lengths of LS2+YETS → Keep RT period as short as possible!!

Conversion from luminosity to Φeq is done via the measurement of leakage current. 25% error estimated along Z coordinate.

TCAD simulation of silicon detectors: A validation tool for the development of LGAD
Marco Mandurrino

By validating models and simulations on available data we intend to obtain a predicting tool allowing to design new generations of radiation-resistant LGAD devices

Compared 3 different avalanche models to measured data, for different fluences and T
Included recently observed acceptor removal effect.
Radiation effects via 3-level Perugia model

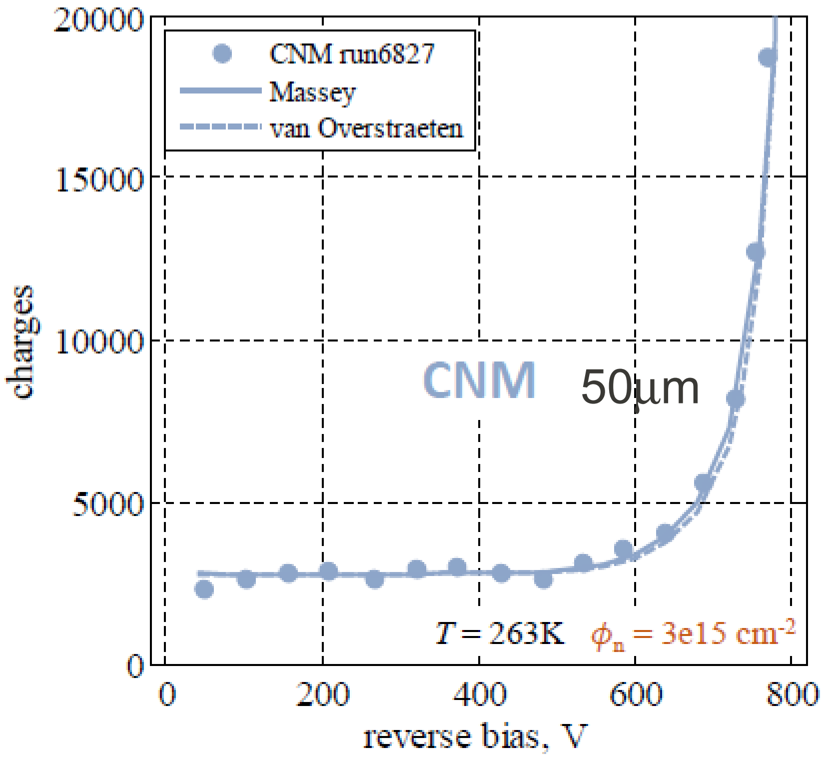

Pin simulation

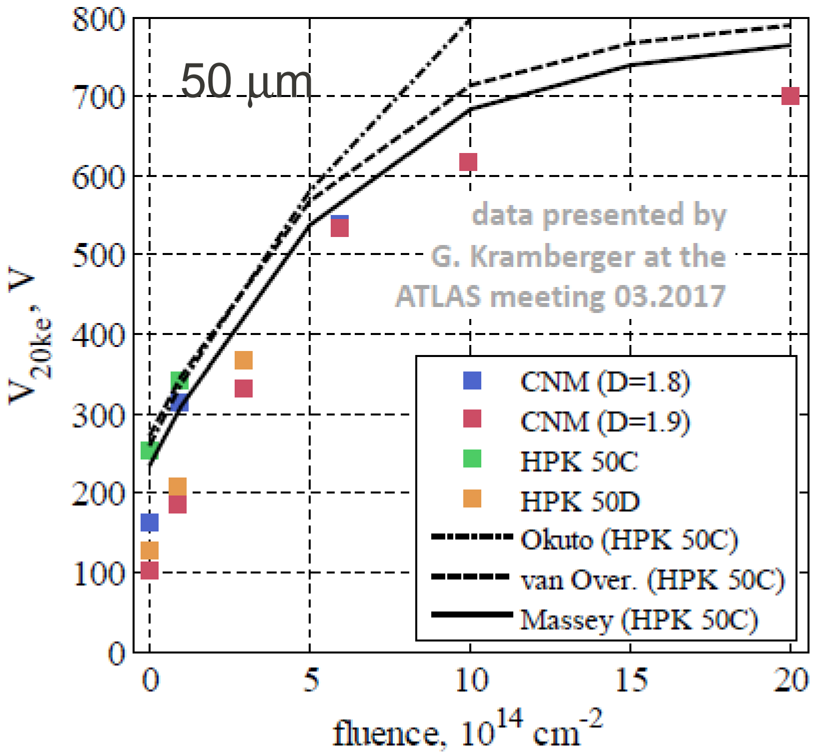

data presented by G. Kramberger at the ATLAS meeting 03.2017

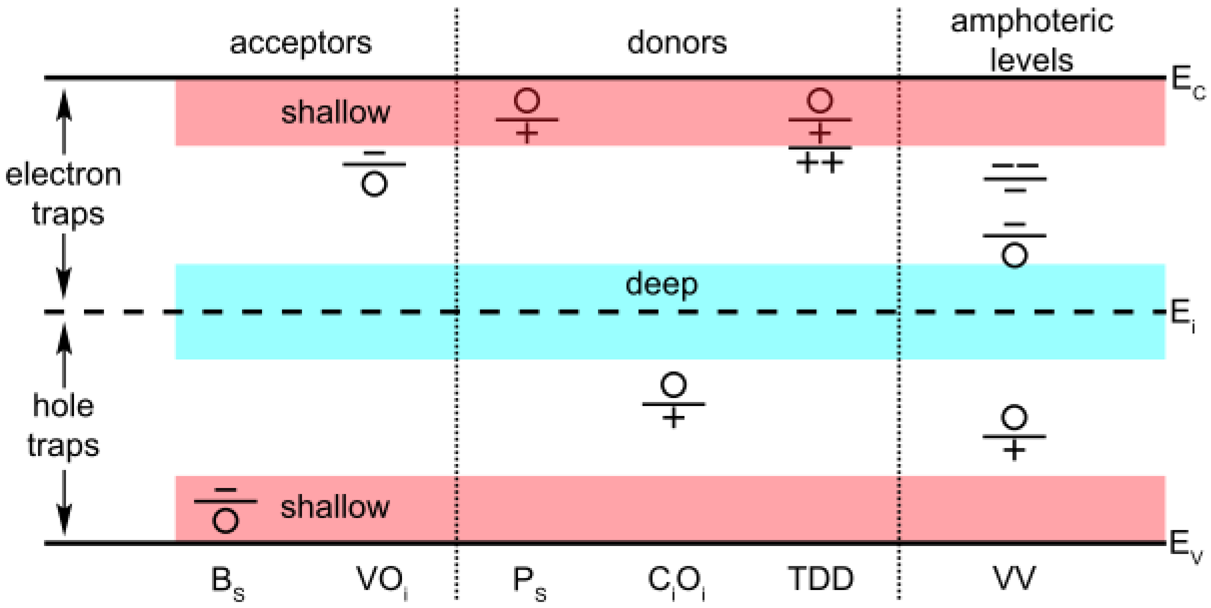

=Energy reference

Levels usually not filled by e

Levels usually filled by e

Figure 4.3.1.: Illustration of possible charge states of defects in the band gap. Figure reproduced from [32]. The labelling of charge states of defects follows this graphical representation. Information about the defects see chapter 7.

An **acceptor** is neutral if empty and negative if filled by an electron

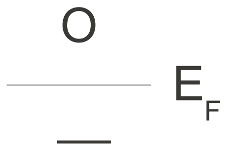

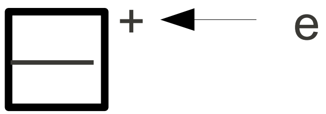

A **donor** is defined as being neutral if filled by an electron, and positive if empty.

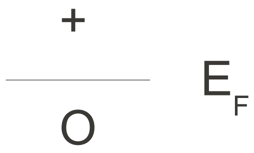

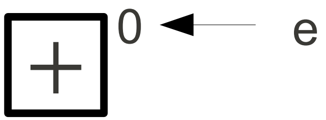

An amphoteric defect has both donor and acceptor states in the band gap

The charge state of a defect level (at least in thermal equilibrium) depends on the relative position to the Fermi level. If located above the Fermi level, acceptors are neutral and donors are positively charged, if the Fermi level is located above the defect level, acceptors are negatively charged and donors are neutral. e. Usually levels in the upper part of the band gap are not occupied with electrons, while defects in the lower part are occupied by electrons

Defects related to change of doping

Defects related to leakage current

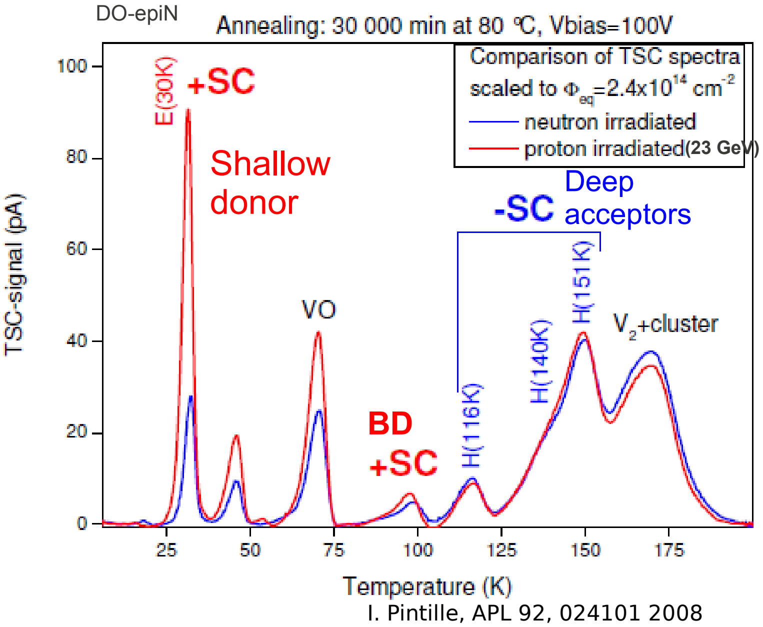

I. Pintille, APL 92, 024101 2008

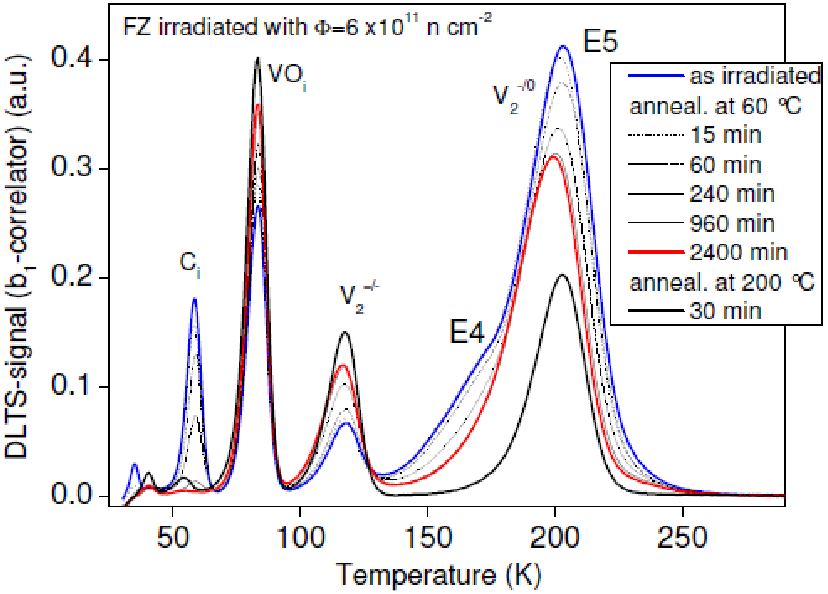

H(116K,140K,151K) defects introduces **negative space charge** (-SC) and are responsible for type inversion of n-type material..

In **Oxygenated** materials **E(30K)** introduces +SC and avoids type inversion.

VP → **Donor Removal** process (suppressed in O-rich material)

$I+B_s \to B_i$
$B_i+O_i \to B_iO_i$ } **Acceptor removal**
(=Positive SC)

Leakage current decreases with annealing time at high T.

DLTS spectra at different annealing stages show **dissolution** of peak at 200K into several defects (**E4** and **E5**) (peak **height** proportional to defect **concentration**). These defects are DLs responsible of leakage current increase.

E5 correlates linearly with fluence

Mapping of defects to sensor performace

Mitigation of radiation **damage** requires Identification and **characterization** of defects responsible for changes in device properties.

This task is **unique to RD50.** No other CERN collaboration/experiment is addressing this problem.

MAcroscopic changes are:

change of effective **doping**
increase of **leakage** current
Trapping of charge carriers

MIcroscopic defects to be linked to macroscopic changes can be:

point defects
induced by 60Co-γ and charged hadrons)
clusters
(charged hadrons and overall neutrons)

Defect characterization methods:

Thermally Stimulated Current (TSC)
Gives concentration of defects.
Can be used for highly irradiated devices
Three steps measurements:
1) **cooling** under reverse bias (keeps traps empty)
2) **Filling** of traps with e and h from forward bias
3) **Heating** under reverse bias and recording current due to carriers released from traps at certain energy (Temperature)

Deep Level Transient Spectroscopy (DLTS)
Gives all the information of defects (c,E_t,N_t)
Limited to Nt << Neff,0=conc of shallow dopants
Principle of operation::
Defect filling by quick reduction (~100 ms) of the reverse bias of a diode. **Charges** are then **emitted** depending on the emission rate of defects. The change of Neff changes the capacitance. Analysis of Capacitance transients gives full information of the defect

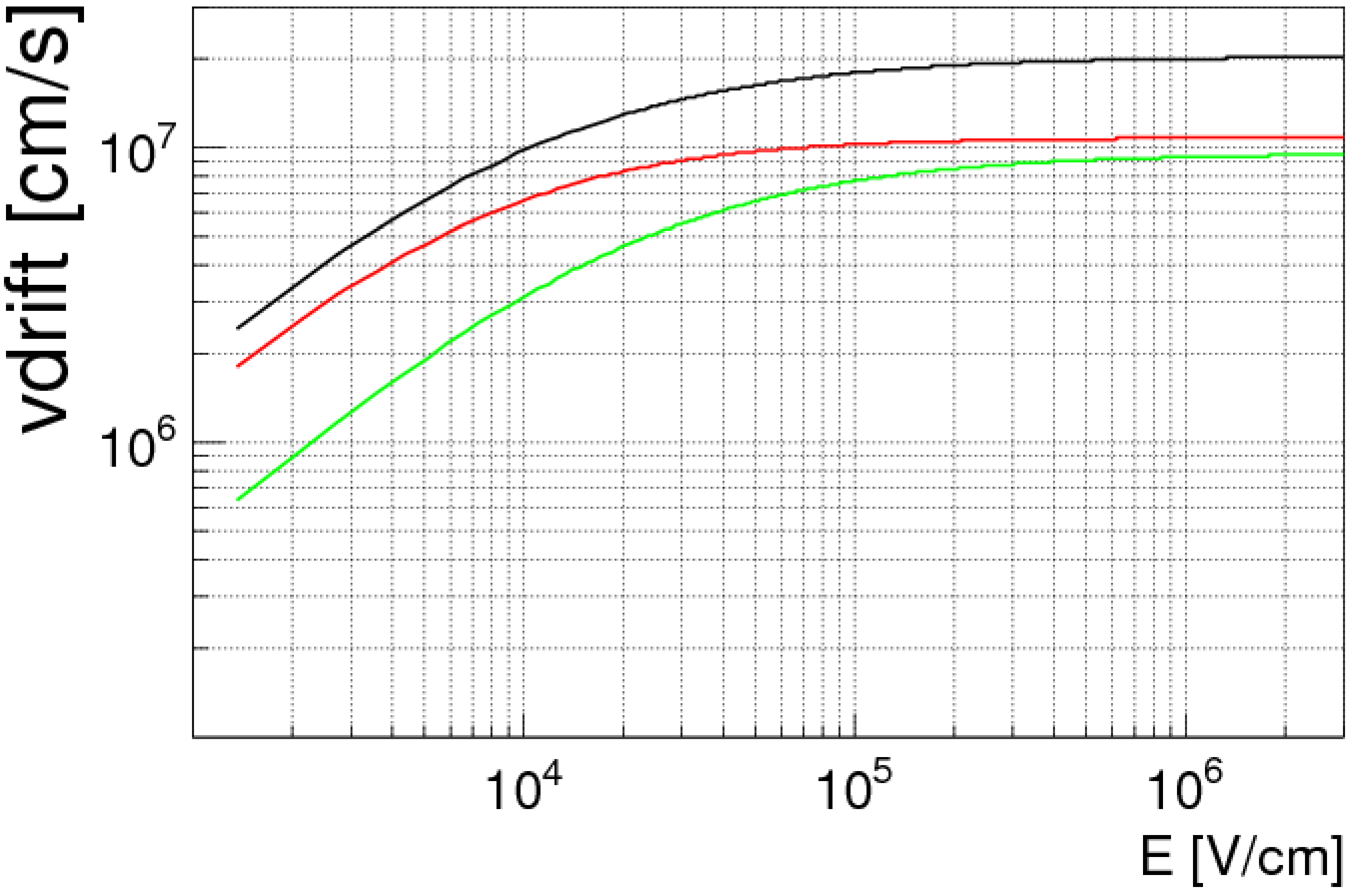
vdrift [cm/s]
10^7
10^6
10^4
10^5
10^6
E [V/cm]

Fabrication

Starting from neutron transmutation n-doped $<100>$ Si wafers

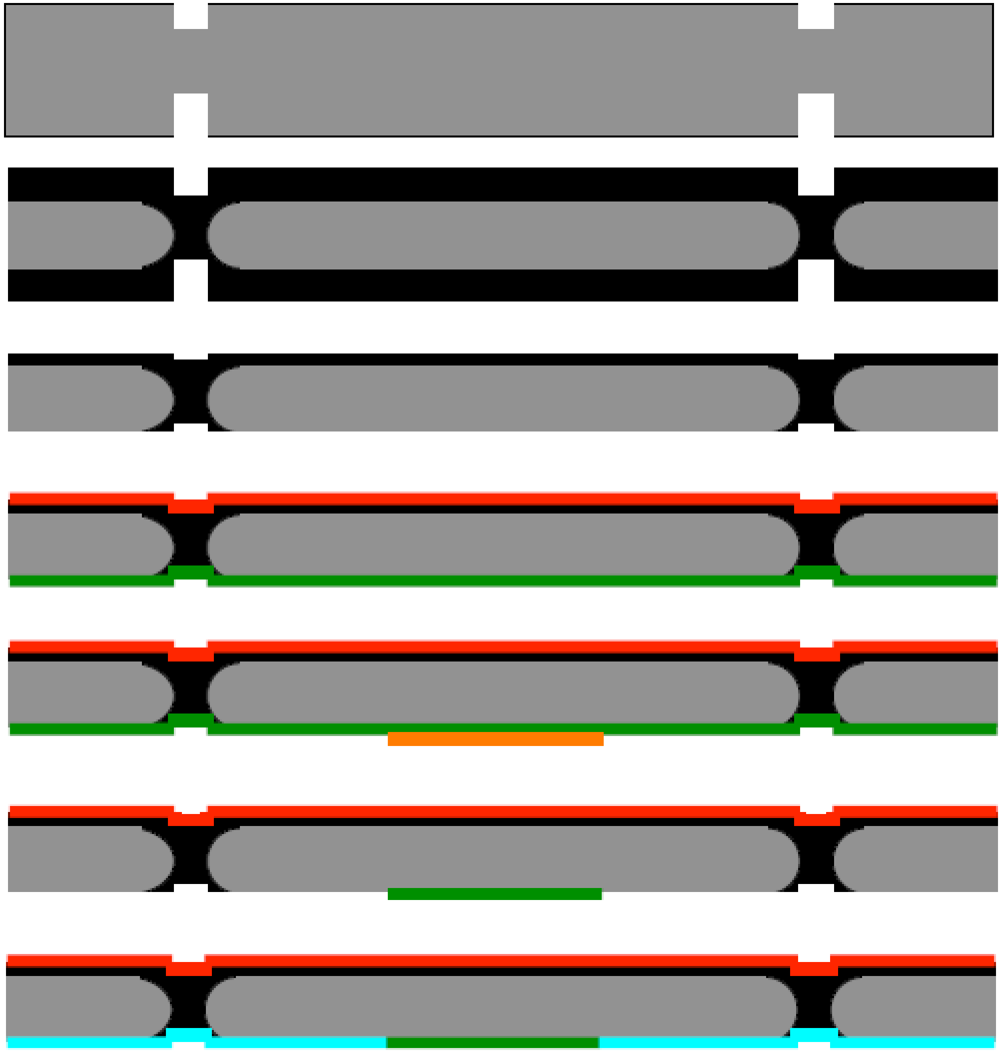

Saw cut grooves added to n-type silicon

Deep p-type diffusion (black)

Polishing defines p-n junction depth

The p$^+$ (red) and n$^+$ (green) layers are diffused into the front and back surfaces

Part of the n$^+$ region is masked with an etch resist polyimide (orange)

The masking polyimide is removed, leaving residual n+ material that forms the contact electrode.

Wafer cleaned. Passivation polyimide applied photolithographically on entire back side except n+ pads.

E. Vilella et al. RD50 HV-CMOS submission in LFoundry 150 nm

Former experience on similar project

Too early BD: 24 V
Two problems identified

1) Parasitic BD

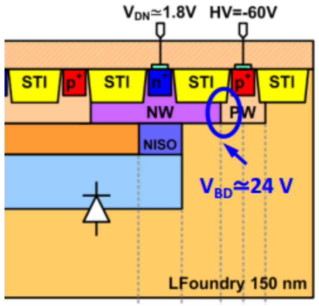

Obtained

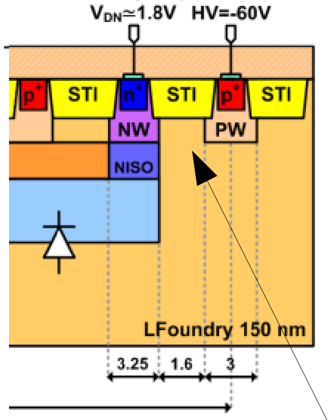

Wished

2) PW/NW separation > 3 um for VBD>75 V→ pixel re-design